POLITECNICO DI MILANO

School of Civil and Environmental Engineering

Polo Territoriale di Como

Master of Science in

Environmental and Geomatic Engineering

Thesis Topic:

Heights datum alignment using global models: Satellite-only GOCE model and EGM2008

Supervisor:

Prof. Fernando Sansò

Assistant Supervisors:

Ing. Daniele Sampietro. PhD.

Ing. Madalena Gilardoni. PhD.

Master's of Science Thesis by: Anthony Osei Tutu;

Matricola: 777241

Academic Year: 2012/2013

Acknowledgement

I would like to express my sincere gratitude to my supervisor Prof. Fernando Sanso, for the immense support and all the time he had for me since the inception of this project. It has been a great impact to my career; given the semester lecturing I had on spherical harmonics and statistics to prepare me for the project.

Special thanks also goes to the entire staff members of the Geomatic group, Polo Territoriale di Como, especially Daniele Sampietro, Madalena Gilardon, Andrea Gatti, Maria Grazie Ballabio,etc. for their support and time. I am very much indebted to you all for the success of my thesis project.

My classmates and friends (Irfan, Parvase, Hoang, Fabio, Matteo,etc.), have been colleagues to remember for the true friendship exhibited in our course of study. These two years wouldn't have been this perfect, if it had not been your sense of responsibility towards me as a friend. I would also like to show my appreciation to my church (Chiesa Cristiana Avventista di Como), for being such a great family for my two years in Como.

My heartfelt thanks go to my parents, Mr Bright Osei Tutu and Mrs Comfort Brago Osei Tutu and my siblings for their love and support during all the years of my studies.

Above all, thanks to the Almighty God for my life.

Abstract

Geoids of different continent or regions have been estimated by different people with different data source and computation procedure. As a consequence they are not completely consistent one to another: usually they have different spatial resolutions, accuracies, and precision. Moreover each may also have been estimated with different datum or reference ellipsoid. For these reasons national geoids of neighboring countries usually do not fit to each other along the borders. Nowadays, thanks to the improvement in the global description of the gravitational field due to dedicated satellite mission it is possible to merge neighboring geoids into a common geoid, taking into account local information. In fact, satellite models are not affected by local biases since they do not make use of any ground gravity data and they are referred to a global geocentric ellipsoid. This alignment of height datums are of much importance in many applications such as international civil engineering works (e.g. Channel for a Tunnel project) and any application that will require the height referencing.

In the present work a merging strategy based on two steps is proposed. Firstly, the bias and the systematic effect due to a variation of the position of centre of the reference ellipsoid are estimated for each national geoid by exploiting GOCE data: using a satellite-only GOCE model, with the assumption that this model is biases-free, the long wavelengths of the local geoids are removed. The remaining signal consists of errors from the local data, i.e. the sum of the bias to be estimated and a white noise (observation error), GOCE model errors and the high frequency part of the signal. This last term, where the effect of the bias is negligible can be removed e.g. by using EGM2008 model. At this point the biases can be estimated by means a least squares adjustment. Three different shapes of the biases were considered, i.e. a constant for each geoid or

a trend for each model considering the origin and the translation of the barycenter or a constant for each geoid and a common trend for all geoids of the translation of the barycenter.

Secondly, these straightened geoids are “sewn” to each other by applying a kriging procedure along the borders. In this way the final result is an unbiased geoid, joining in an optimal way the national models. In order to test the proposed procedure, we have merged the geoids of Italy, Switzerland, French, and part of Germany, Austria, Slovenia, Croatia, and the Mediterranean Sea from the European quasigeoid.

Keywords: GOCE model, EGM2008, height datum unification, bias model, GPS/leveling, Kriging.

Riassunto

Geoidi di continenti o regioni diverse sono stati stimati da persone diverse con diversa dati di origine e procedure di calcolo. Di conseguenza questi geoidi non sono generalmente coerenti tra loro. Infatti i geoidi locali sono forniti a diverse risoluzioni spaziali, accuratezze e precisioni. Inoltre ogni geoide può essere stato con datum o un'ellissoide di riferimento diverso. Per queste ragioni geoidi nazionali di paesi confinanti di solito non si adattano l'uno all'altro lungo i confini. Oggigiorno, grazie al miglioramento nella descrizione globale del campo gravitazionale dovuta alla missione satellitare GOCE è possibile unire geoidi confinanti in un geoide comune, tenendo conto delle informazioni locali. Infatti i modelli satellitari non sono influenzati da sistematismi locali, dal momento che non fanno uso di dati gravimetrici a terra e si riferiscono a un'ellissoide geocentrico globale. L'allineamento di datum altezza è di grande importanza in molte applicazioni, come ad esempio le opere di ingegneria civile internazionali (canali, gallerie, etc.) e qualsiasi applicazione che richieda la conoscenza di altezze ortometriche.

Nel presente lavoro si propone una strategia di fusione basata su due fasi. Innanzitutto, il bias e i sist3ematismi dovuti ad una variazione della posizione del centro dell'ellissoide di riferimento sono stimati per ciascun geoide nazionale sfruttando dati GOCE. Utilizzando un modello GOCE-only, le lunghezze d'onda dei geoidi locali possono infatti essere rimossi. Il segnale residuo costituito dagli errori dei modelli locali, cioè la somma dell'errore di stima del bias e un rumore bianco (errore di osservazione), errori del modello GOCE e la parte ad alta frequenza del segnale. Quest'ultimo termine, dove l'effetto della distorsione è trascurabile può essere rimosso ad esempio utilizzando il modello EGM2008. A questo punto i parametri del bias possono essere stimati mediante una compensazione ai minimi quadrati. In particolare tre differenti "forme" di

bias sono stati considerati: una costante per ogni geoide, una costante più un trend per ogni geoide nazionale o una costante per ogni geoide e un trend comune per tutti i geoidi.

In secondo luogo, questi geoidi "unbiased" sono stati uniti tra di loro mediante l'applicazione di una procedura di kriging lungo i confini. In questo modo il risultato finale è un geoide unbiased, che unisce in modo ottimale i modelli nazionali. Al fine di testare la procedura proposta, sono stati uniti i geoidi italiano, svizzero, francese, e il geoide europeo (in parte della Germania, dell'Austria, della Slovenia, della Croazia e del Mar Mediterraneo).

Parole chiave: modello GOCE, EGM2008, unificazione datum d'altezza, modelli di bias, GPS/leveling, Kriging.

Table of Contents

List of Figures

List of Tables

Chapter 1

1.0 Geodesy

1.1 Introduction

Physical geodesy is the study of the physical properties of the gravity field of the Earth, the geopotential, with a view to their application. The estimation of geoid (equipotential surface of the Earth's gravity field) with high accuracy is the main goal among scientist in the geodesy community. GPS will meet its target of accuracy in height component determination (orthometric height) upon obtaining very high accurate geoid, easing high cost of leveling in engineering applications. This will be of great achievement in positioning, oceanography, geophysical applications and most engineering works. Geoids of different countries shearing border do exhibit discontinuities at the boundaries. These jumps at the borders, that are not physical, can be attributed to a number of processes; among them are different reference ellipsoids for geoid estimation, varying spatial resolutions, different accuracies, and different data sources. The effects of those in-homogeneities are usually long wavelength errors called biases. Therefore to align geoids requires the proper estimation of the inherent biases. The proposed bias estimation process is done by basically removing from local geoids the low frequencies, remaining the very high frequencies due to topography, using global satellite-only gravity field models. These models, usually delivered as coefficients of a spherical harmonic series (Heiskanen and Moritz 1967), being computed globally from a homogeneous (both in space and accuracy) dataset and referred to a unique reference ellipsoid can be considered bias-

free. In this work the various local geiods meeting at the European Alps region, i.e. the Italian (Barzaghi et al. 2007), French (Duquenne et al. 1997), Swiss (Marti et al. 1998), and European (Denker et al. 1997) models covering part of Austria, Germany, Slovenia, Croatia and the Mediterranean Sea; figure1.1, with different resolutions and accuracies are used to estimate a new geoid (height datum).

Figure 1.1: Area of Height Datum alignment

1.2 The Earth Gravity field

The total force acting on a body at rest on the Earth's surface is the gravitational force and the centrifugal force due to the Earth's rotation and is call gravity. Assume a rectangular coordinate system whose origin is at the center of the Earth gravity field and whose z-axis coincides with the Earth's mean axis of rotation. The x- and y-axes are so chosen as such that they are at right-angle to each other, with the x-axis intersecting the mean equatorial plane, and as well perpendicular to the z-axis. See figure 1.2.

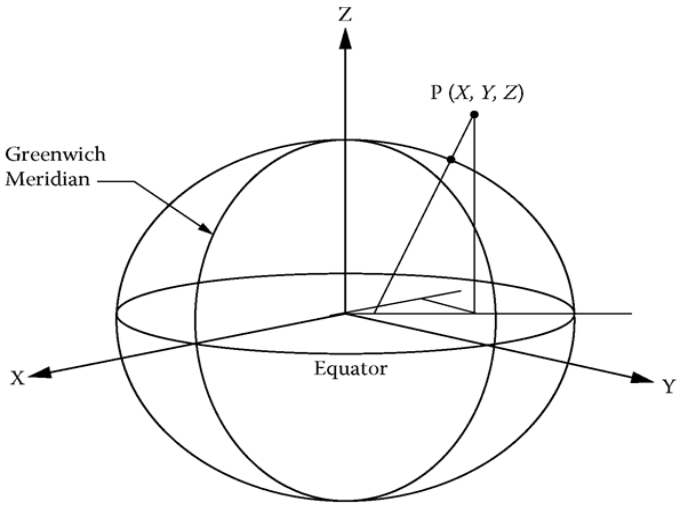

Figure 1.2: Coordinate system

We further assume the Earth to be a solid body rotating with constant speed around a fixed axis – z. An in-depth to this assumption is given by Moritz Mueller (1987). The Earth's motion affects everything on its surface by a resultant force of gravitational force, centrifugal force, and Coriolis force. The Coriolis force acts on a moving body and it is proportional to its velocity with respect to the Earth, so that a body resting on the Earth, it is zero. The centrifugal force *f* on a unit mass is given by: the direction of the vector p = [x, y, z] for z = 0,

$$\boldsymbol{f} = \boldsymbol{w^2 p} \tag{1.1}$$

$$\boldsymbol{\rho} = \sqrt{\boldsymbol{x^2 + y^2}} \tag{1.2}$$

Where $\boldsymbol{w}$ is the angular velocity of the Earth's rotation and $\boldsymbol{\rho}$ is the distance from the rotation axis. The centrifugal force can also be derived from a potential (see e.g. Sansò and Sideris 2013):

$$\Phi = \frac{1}{2}\, w^2\, (x^2 + y^2) \qquad \text{so that} \qquad f = \text{grad}\Phi \equiv \left[\frac{d\Phi}{dx}, \frac{d\Phi}{dy}, \frac{d\Phi}{dz}\right] \tag{1.3}$$

Newton's law of gravitation predicts that, two masses separated by a distance *l* attract each other with a force called gravitational force F, with a potential $V(P)$ on the body at point P.

$$F = \nabla V \qquad \text{where } V(P) = G \iiint_v \frac{p}{l} d_v \qquad \textbf{(1.4)}$$

where G is Newton's gravitational constant (G = 66.7x10-9 cm3 g-1 s-2),

l is the distance between the masses *dm =pdv*,

p the density of the element of volume *dv* and

v the Earth volume.

Gravity is the resultant of gravitational force and centrifugal force. Accordingly, the potential of gravity, *W*, is the sum of the potentials of gravitational force, *V* (1.4) and centrifugal force, Φ (1.3) (Hofmann-Wellenhof and Moritz 2006):

$$W = V + \Phi = G \iiint_v \frac{p}{l} d_v + \frac{1}{2} w^2(x^2 + y^2) \qquad \textbf{(1.5)}$$

The corresponding gravity potential in spherical coordinates is

$$W = \sum_{n=0}^{+\infty} \sum_{m=-n}^{n} Anm \frac{Ynm_{(\theta,\gamma)}}{r^{n+1}} + \frac{1}{2} w^2 r^2 sin\theta \qquad \textbf{(1.6)}$$

The direction of the gravity vector is the direction of the plumb line, or the vertical. The first derivative of *V*, that is the force components, is continuous throughout space, but not the second derivatives; the potential *V* satisfies Poisson's equation, with a Laplace operator Δ:

$$\Delta V = -4\pi G p \qquad \forall p\pi \in v \qquad \textbf{(1.7)}$$

$$\Delta V = \frac{d^2 v}{dx^2} + \frac{d^2 v}{dy^2} + \frac{d^2 v}{dz^2} \quad ; \qquad \text{where } \Delta = \frac{d^2}{dx^2} + \frac{d^2}{dy^2} + \frac{d^2}{dz^2}$$

Outside the attracting bodies, in an empty space, the density is zero, hence the potential V satisfies the Laplace's Equation, (1.6).

$$\Delta V = 0. \quad \textbf{(1.8)}$$

The solutions are called harmonic functions. The potential of gravitation is a harmonic function outside the attracting masses but not inside the masses: there it satisfies Poisson's equation. As any harmonic function, in the harmonic domain Ω, V can be expanded in terms of spherical harmonics Y_{nm} (θ, λ), using spherical coordinates (r, θ, λ) (see for instance Colombo 1981; Reguzzoni 2004).

$$V(P) = G \sum_{n=0}^{+\infty} \sum_{m=-n}^{n} \frac{Y_{nm}(\theta,\lambda)}{r^{n+1}} V_{nm} \quad \textbf{(1.9)}$$

Where $V_{nm} = \frac{k}{2n+1} \iiint_v \rho r'^n Y_{nm(\theta',\lambda')dv}$

$$Y_{nm}(P) = Y_{nm}(\mathrm{r},\theta,\lambda) = \frac{a^n}{r^{n+1}} P_{nm} \sin(\theta) \begin{cases} \cos m\lambda, 0 \le m \le n \\ \sin m\lambda - n \le m \le 0 \end{cases} \quad \textbf{(1.10)}$$

a is semi-major axis of the Earth and

P_{nm} are the associated Legendre Polynomial functions.

1.3 Anomalous Potential

The anomalous potential or disturbing potential T, is defined as the difference between the actual potential $W(p)$ and the normal gravity potential $U(p)$. It is given by:

$$T(p) = W(p) - U(p) \quad \textbf{(1.11)}$$

Since *W(P)* and *U(P)* have the same centrifugal potential, *T(P)* may be seen as the difference between the actual gravitational potential *V* and the normal harmonic component. Therefore, *T* depends on the ellipsoid *E* to which *U(P)* is attached.

$$T(p) = V(p) - V_o(p) \quad \textbf{(1.12)}$$

$$\Delta T(p) = \Delta V(p) = -4\pi\rho(p) \quad \textbf{(1.13)}$$

And outside the surface,

$$\Delta T(p) = 0 \; \Delta T \quad \textbf{(1.14)}$$

Hence, it can be expanded into a series of spherical harmonics (1.15). The anomalous potential *T* is $10^{-5} - 10^{-6}$ times smaller than *U*, so it can be used as an infinitesimal quantity of the first order in a linearization process. An important geometric quantity related to the anomalous field is the geoid undulation *N*, the distance along the normal to the ellipsoid *n'*, between a point p on the geoid and Q on the ellipsoid.

$$T(r,\theta,\lambda) = \sum_{n=2}^{\infty} \sum_{m=-n}^{n} T_{nm} \left(\frac{R}{r}\right)^{n+1} Y_{nm}(\theta,\lambda) \quad \textbf{(1.15)}$$

1.4 The Gravimetric geoid determination

The geoid can be estimated by a number of mathematical processes in which the anomalous potential T is estimated from the function in a harmonic domain. Several solutions to this problem are known in geodetic literature, such as the localization" of Molodensky's theory (Molodensky et al. 1962), the Taylorizing of global models to local data (e.g. Wenzel 1982, Kearsley and Forsberg 1990, Reguzzoni et al. 2011), the Stokes-Helmert approach (Stokes 1849)

and its variants (between the others, Vanicek and Sjoberg 1991, Martinec and Vannicek 1994, Heck 2003, Novak 2007) the collocation approach (Moritz 1980, Sansò 1986, Tscherning 1994, Krarup 2006) with its particular form of the remove-restore principle (Forsberg 1994) or more recently a method based on radial basis functions (Klees et Al. 2008).

Approximating the geoid estimation can be followed by the remove restore concept, and applying either Stokes boundary problem or Least squares collocation procedure:

$$\Delta g - \Delta g_m - \Delta g_{rtc} = \Delta g_r$$

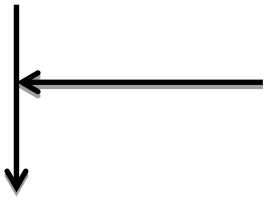

Stokes /Collocation procedure **(1.16)**

$$T = T_m + \Delta T_{rtc} - \delta T_r$$

1.4.1 Stokes' Boundary Value problem

$$\Delta g = -\frac{\partial T}{\partial r} - \frac{2}{r}T \qquad \textbf{(1.17)}$$

The equation 1.17 can only be regarded as a boundary condition, as long as the gravity anomaly Δg is known only at the surface of the Earth. However, by upward continuation, the gravity anomalies outside the Earth can be computed. This makes the equation a real differential equation that can be integrated with respect to the distance *r*, and in addition satisfies Laplace's equation ΔT = 0 (Sansò and Sideris 2013).

The differential becomes $-r^2\Delta g = r^2\frac{\partial T}{\partial r} + 2rT = \frac{\partial}{\partial r}(r^2T)$ **(1.18)**

and the integral form is given by; $\frac{\partial}{\partial r}(r^2T) = -r^2\Delta g(r)$ **(1.19)**

Between the limits ∞ and r we find

$$r^2T = -\int_{\infty}^{r} r^2\Delta g(r)dr \quad \textbf{(1.20)}$$

where Δg(r) indicates that Δg is a function of r, computed from the surface gravity anomalies. The evaluation of the potential here is estimated from degree two of the spherical harmonics, omitting the degrees one and zero as the anomalous potential can contain such terms. From the integration with respect to *r*, the potential *T* given by Pizzetti's formula is

$$T(r,\vartheta,\lambda) = \frac{R}{4\pi}\iint_{\sigma} S(r,\psi)\Delta g d\sigma \quad \textbf{(1.21)}$$

Therefore the Stokes' formula is given by; $T = \frac{R}{4\pi}\iint_{\sigma} \Delta g S(\psi) d\sigma$ **(1.22)**

By Burns' theorem, $N = T/\gamma_o$, we get the Stokes integral as

$$N = \frac{R}{4\pi\gamma_o}\iint_{\sigma} \Delta g S(\psi) d\sigma \quad \textbf{(1.23)}$$

where S (ψ) is the Stokes' function.

The Stokes' function expressed in terms of Legendre polynomials is given by (Hofmann-Wellenhof and Moritz 2006):

$$S(\psi) = \sum_{n=2}^{\infty} \frac{2n+1}{n+1} P_n(\cos\psi). \quad \textbf{(1.24)}$$

1.4.2 Collocation

In Geodesy, the collocation method can be applied to the estimation of any linear function example, the anomalous potential *T(P),* given observed values which are themselves linear

functions of *T(P)* (Moritz, 1980). The anomalous potential *T* outside the Earth is a harmonic function, which satisfies Laplace's differential equation

$$\Delta T = \frac{\partial^2 T}{\partial x^2} + \frac{\partial^2 T}{\partial y^2} + \frac{\partial^2 T}{\partial z^2} = 0 \quad \textbf{(1.24)}$$

By the remove restore concept, the quantities Δg_M and T_M are removed from the corresponding Δg and T, such that the remaining fields have a comparatively higher power in medium and high frequency part of the spectrum. The residual terrain correction Δg_{RTC} is also estimated for the topographic effects from the gravity anomaly. The evaluation of the pure residual field and its corresponding potential from real data Δg is given by (Sanso, 2000):

$$\Delta g_R = \Delta g - \Delta g_M - \Delta g_{RTC} \quad \textbf{(1.25)}$$

$$T_R(p) = T(p) - T_M(p) - T_{RTC}(p) \quad \textbf{(1.26)}$$

From equation (1.25) the resulting empirical covariance function $C_{\Delta gR\Delta gR}(\psi)$ is computed, then the covariance and the cross covariance below is computed.

$$C_{TT}(\psi_{pq}) = \left(\frac{\mu}{R}\right)^2 \sum_{n=2}^{+\infty} \sigma_n^2 (T) \left(\frac{R^2}{r_p r_q}\right)^{n+1} (2n+1) P_n(\psi_{pq}) \quad \textbf{(1.27)}$$

$$C_{\Delta gR\Delta gR}(\psi_{pq}) = \left(\frac{\mu}{R^2}\right)^2 \sum_{n=2}^{+\infty} \sigma_n^2 (T) \left(\frac{R^2}{r_p r_q}\right)^{n+2} (n-1)^2 (2n+1) P_n(\psi_{pq}) \quad \textbf{(1.28)}$$

$$C_{\Delta gT}(\psi_{pq}) = \left(\frac{\mu}{R}\right)\left(\frac{\mu}{R^2}\right) \sum_{n=2}^{+\infty} \sigma_n^2 (T) \left(\frac{R}{r_p}\right)^{n+2} \left(\frac{R}{r_q}\right)^{n+1} (2n+1)(n-1) P_n(\psi_{pq}) \quad \textbf{(1.29)}$$

Now to estimate $\hat{T}$ (P) from Δg (Pi) (i = 1, 2, ……, N), an average estimation error is done, to be evaluated in the class of linear functions of the observations,

$$\begin{cases} \varepsilon^2 = E\left\{\left[T(P) - \hat{T}(P)\right]^2\right\} \\ T(P) = \sum_{i=1}^{N} \lambda_i \Delta g(P_i) \end{cases} \quad \textbf{(1.30)}$$

resulting in

$$\varepsilon^2 = C_{TT}(0) - 2\sum_{i=1}^{N} \lambda_i C_{T\Delta g}(P_i P_i) + \sum_{ij=1}^{N} \lambda_i \lambda_i C_{\Delta g \Delta g}(P_i P_i) \quad \textbf{(1.31)}$$

Minimizing the equation (1.30), with respect to λi, both T(P) and its estimation error are ε evaluated as,

$$\begin{cases} \hat{T}(P) = \sum_{ij=1}^{N} C_{T\Delta g}(P_i, P_i) C^{-1}_{\Delta g \Delta g}(P_i, P_j) \Delta g(P_i) \\ \varepsilon^2 = C_{TT}(0) - C_{T\Delta g}(P_i, P_i) C^{-1}_{\Delta g \Delta g}(P_i, P_j) C_{\Delta g T}(P_j, P_j) \end{cases} \quad \textbf{(1.32)}$$

The collocation technique is evaluated with equations (1.32), assuming data with no noise. Though all measured data has some level of systematic noise which is evident by comparing the empirical and model covariance functions in the origin;

$$C_{emp}(0) C_{mod}(0) = \sigma_v^2 > 0 \quad \textbf{(1.33)}$$

1.5 The Geoid

The surface of constant gravity potential, w_o that closely approximates mean sea level is known as the geoid. If the constant normal gravity potential, U_0, on the normal ellipsoid is equal to the constant gravity potential of the geoid, then the gravity anomaly on the geoid is the difference between gravity on the geoid and normal gravity on the ellipsoid at respective points, P_0, Q_0, sharing the same perpendicular to the ellipsoid. The separation between the geoid and the ellipsoid is known as the geoid undulation, N or also geoid height (Figure 1.3). A simple Taylor

expansion of the normal gravity potential along the ellipsoid perpendicular yields the following important formula:

$$N = \frac{T}{\gamma} \qquad \textbf{(1.34)}$$

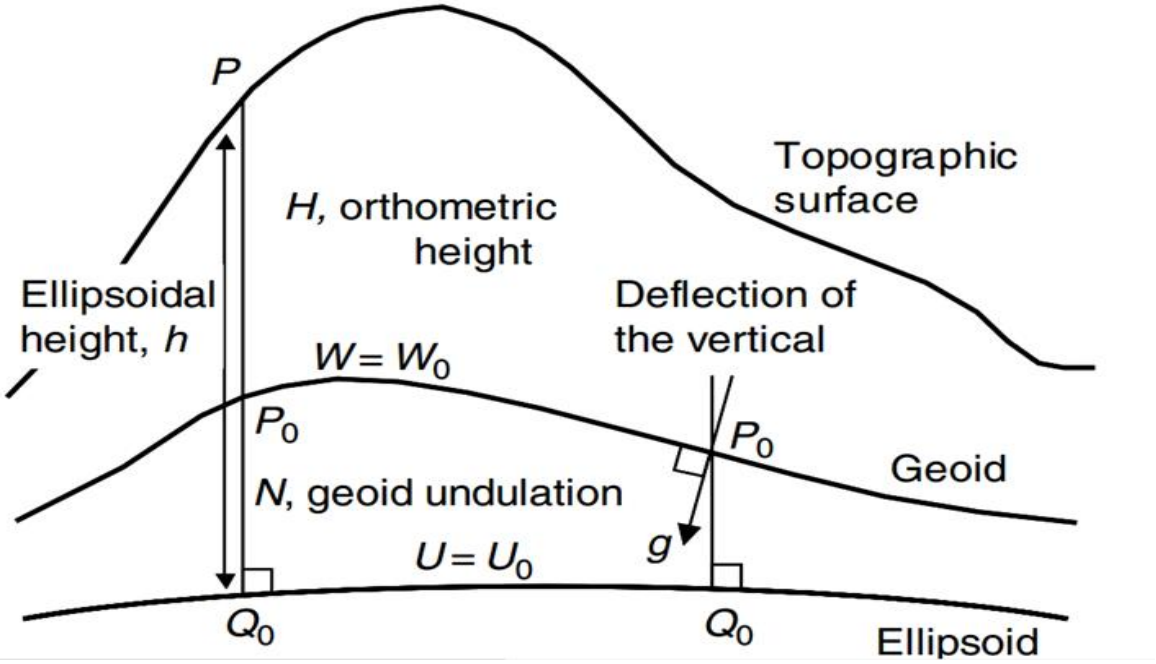

Figure: 1.3 The Geometry of the ellipsoid, geoid and the topography

This is Bruns' equation (1.34), which is accurate to a few millimeters in N, and which can be extended to $N = T/\gamma - (W_0 - U_0)/\gamma$ for the general case, $W_0 \neq U_0$. The gravity anomaly (on the geoid) is the gravity disturbance corrected for the evaluation of normal gravity on the ellipsoid instead of the geoid. This correction is $N = d\gamma/dh = (d\gamma/dh)(T/\gamma)$, where h is height along the ellipsoid perpendicular. We have $\delta g = \frac{\delta T}{\delta h}$ and hence

$$\Delta g = -\frac{\partial T}{\partial h} + \frac{1}{\gamma}\frac{\partial \gamma}{\partial h} T \qquad \textbf{(1.35)}$$

The slope of the geoid with respect to the ellipsoid is also the angle between the corresponding perpendiculars to these surfaces. This angle is known as the deflection of the vertical, that is, the deflection of the plumb line (perpendicular to the geoid) relative to the perpendicular to the normal ellipsoid. The deflection angle has components, ξ, η, respectively, in the north and east directions. The spherical approximations to the gravity disturbance, anomaly, and deflection of the vertical are given by

$$\delta g = -\frac{\delta T}{\delta r}, \qquad \Delta g = -\frac{\partial T}{\partial r} - \frac{2}{r} T \tag{1.36}$$

$$\xi = \frac{1}{\gamma} \frac{\partial T}{r \partial \theta} \qquad = -\frac{1}{\gamma} \frac{\partial T}{r \sin\theta \partial \lambda} T \tag{1.37}$$

where the signs on the derivatives are a matter of convention (Jekeli, 2007).

Chapter 2

2.0 Height Systems and Vertical Datums

2.1. Height System

There are numerous height systems which are established for different purposes. Most of these heights are related to the Earth's gravity field or an approximation of it. (e.g. Featherstone and Kuhn, 2006; Hannah, 2001; Heiskanen and Moritz, 1967). Here, the various height systems are discussed and with particular attention on the way they are used in the definition of a vertical datum.

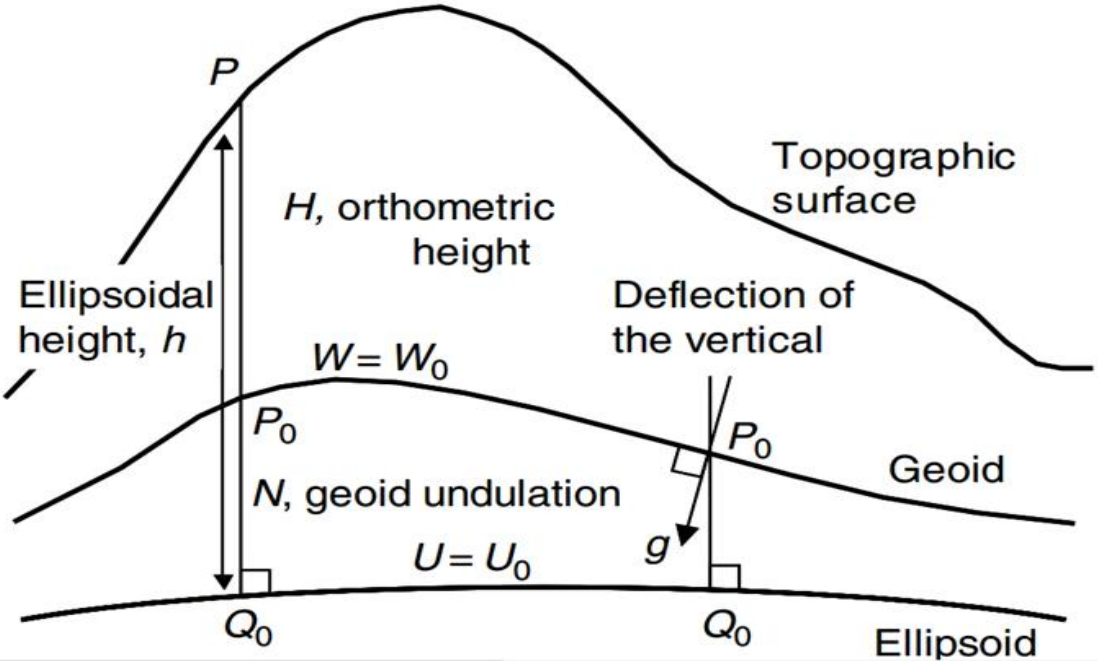

Figure 2.1: Heights relations

2.2. Geopotential number

Strictly, all natural or physical height systems must be based on geopotential numbers, C (Heiskanen and Moritz, 1967). A geopotential number is the difference in potential from a reference equipotential surface, W_0, (usually the geoid) to the potential at the point of interest, W_P, where P is the point of interest; P_0 is the corresponding intersection of P with the geoid along the plumb line; and g is the gravity vector along the plumb line (see figue 2.1), dz.

$$C = W_0 - W_p = \int_{po}^{p} g\,dz \quad \text{(Heiskanen and Moritz, 1967)} \qquad \textbf{(2.1)}$$

Geopotential numbers are measured in geopotential units (GPU), where 1 GPU = 10 m^2s^{-2}. Because they do not have units of length, they are less intuitive to non-technical users. They accurately predict the flow of water (water will flow from a higher geopotential number to a lower one based on laws of physics and potential theory) and provide a theoretical zero of a close loop regardless of the leveling route taken, i.e. holonomity (e.g., Heiskanen and Moritz, 1967, Sansò and Vanícek, 2005). They are determined using geopotential differences C that are derived from precise leveling and gravity observations (Torge, 2001).

$$\Delta C = g_{mean}\, dn \qquad \textbf{(2.2)}$$

Where g_{mean} is the average surface gravity value and *dn* is the difference in height (both along the precise leveling route). The requirement for surface gravity observations is common to most types of height.

2.3. Dynamic Heights

To overcome the intuitive problem with geopotential numbers not being expressed in units of length, the dynamic height, H^{dyn}, was proposed by Helmert (1884). These heights are obtained by dividing the geopotential number by a constant gravity value, g_0, often chosen to be the value of normal gravity, γ, at 45°. The dynamic height is given by:

$$H^{dyn} = \frac{C}{g_0} \tag{2.3}$$

Dynamic heights are very simple to compute (if the geopotential number is known), because they retain the same characteristics as the geopotential number, predict the flow of fluids correctly. Its unit of length changes depending on the gravity constant used and so it is therefore generally not the same. The dynamic height does not have a geometrical meaning because it is a purely physical quantity (e.g., Heiskanen and Moritz, 1967; Jekeli, 2000). These heights are typically obtained by applying a dynamic correction to spirit levelled height differences. These corrections can be very large if g_0 is not representative of the region concerned (Amos, 2007).

2.4. Orthometric Heights

The orthometric height, H, is defined as the length of the curved plumbline from a point, P, to its intersection with the geoid, P_0, as shown in Figure 2.1 and is given by:

$$H = \frac{C}{g} \tag{2.4}$$

Where $\overline{g}$ is the integral mean value of gravity along the plumbline and is given by:

$$\overline{g} = \frac{1}{H}\int_0^H g(z)dz \qquad \textbf{(2.5)}$$

To determine g, the exact path of the plumbline through the Earth and also the gravitational acceleration at all points along that plumbline need to be known. This requires knowledge of gravity variations or the mass-density distribution (Allister and Featherstone, 2001) through the topography (Dennis and Featherstone, 2003; Featherstone and Kuhn, 2006).

2.5 Normal Heights

The normal gravity field is defined as the gravity field defined by an Earth-fitting ellipsoid that contains the total mass of the Earth (including its atmosphere) and rotates with a constant angular velocity more or less equivalent to that of the Earth (Moritz, 1980a). The normal gravity field can be used to define a height that avoids the density hypothesis for the crust. The normal height (HN) was proposed in 1954 by Molodensky (Molodensky et al., 1962). It replaces g in Equation (2.4) with normal gravity measured along the curved ellipsoidal normal (of the reference ellipsoid), g, hence (Jekeli,2000):

$$H = \frac{C}{\overline{\gamma}} \qquad \text{Where} \quad \overline{\gamma} = \frac{1}{H}\int_0^H \gamma(h)dh \qquad \textbf{(2.6)}$$

It is defined geometrically as the distance along the ellipsoidal surface normal from the reference ellipsoid to the telluroid. The telluroid was defined by Molodensky as the surface whose normal potential, U, at every point, Q, is equal to the actual potential, W, at the corresponding surface point, P, or UQ= WP. The distance between P and the telluroid, Q, is called the height anomaly, this is related to the ellipsoidal height, h, by:

$$\xi = h - H \quad \textbf{(2.7)}$$

Normal heights are simple to compute because they do not require knowledge of the internal mass-density structure of the Earth; this is a virtue of Molodensky theory. The height anomaly is also defined as the distance between the ellipsoid and the quasigeoid; hence the normal heights can be compatible with GPS heights when they are derived from the quasigeoid. Because normal heights do not have any physical meaning (being defined by a gravity model), they are not as applicable to the real Earth as the orthometric height, additionally they cannot universally predict fluid flows (Featherstone and Kuhn, 2006).

2.6 Ellipsoidal Heights

The ellipsoidal height (h) is the distance from the reference ellipsoid to the Earth's surface along the ellipsoidal surface normal as shown in Figure 2.1. Unlike the heights discussed in the Sections above, it is defined independently of the Earth's gravity field, i.e., it is a purely geometric quantity. Consequently, ellipsoidal heights cannot reliably predict the flow of fluids. They are however relatively easy to define mathematically and as such are the type of height obtained from GNSS receivers (such as GPS). Ellipsoidal heights are related to orthometric heights by H = h-N and the normal and normal-orthometric heights by H^N = h - ξ = - and H^{N-O} = h – ξ. Therefore, the difference between the geoid and quasigeoid is given by N – ξ.

2.7 Vertical datum definition

To realise a vertical datum, it is necessary to select a type of height system and a compatible reference surface. Once these choices are made, and the observed height differences have been corrected for systematic errors affecting their observation (e.g. Vanícek et al., 1980). A vertical datum can be realised point-wise by performing a least-squares adjustment of the corrected height differences to minimise the impact of random errors and to account for the non-holonomity of the levelling loops (e.g. Sansò and Vanícek, 2005). Ideally this adjustment should be performed on either the geopotential numbers or on the height differences in a height system that exhibits holonomity (e.g., Featherstone and Kuhn, 2006; Sansò and Vanícek, 2005). However, this is not always possible (e.g., due to the unavailability of gravity observations or the corrections being imperfect). Furthermore, if the heights of multiple points are constrained in the adjustment, then they should all be on the same equipotential surface. If they are not (e.g., where local MSL is fixed at multiple locations around an island or continent), then the vertical datum will be distorted and not represent an equipotential surface over its extents (cf. Featherstone, 2004). The type of height system chosen normally depends on the data that was available to the group responsible at the time of datum. For example, if gravity observations are unavailable, then only the normal-orthometric or ellipsoidal height systems can be used. The choice of reference surface is guided by the choice of height system, i.e. orthometric heights use the geoid; normal heights the telluroid; normal-orthometric heights the quasigeoid and ellipsoidal heights the ellipsoid.

While it is possible to obtain ellipsoidal heights from GNSS technology, it is not currently possible to directly observe the vertical datum surface in natural/physical height systems (e.g.

Featherstone and Kuhn, 2006). Using the assumption that the geoid/quasigeoid and mean sea-level (MSL) in the open oceans are coincident it is possible to relate a vertical datum to the geoid/quasigeoid using local MSL observations.

Vertical datum can also be defined by computing the geopotential number of the origin point using its ellipsoidal height (from GNSS observations) and absolute gravity value. This approach is well-suited to for the connection of continental height datums (i.e. across large water bodies) and is analogous to the geopotential number method of datum unification (Amos, 2007).

2.7 Mean sea-level (MSL)

In the ideal situation, the datum surface (i.e. zero height) of a height system will coincide with the geoid (true orthometric height system) or quasigeoid (normal-orthometric height system). Because there is no instrument that can directly measure the absolute value of the Earth's geopotential, it is not possible to physically observe the geoid. Recall that over the oceans the geoid and quasigeoid are coincident and that they represent an equipotential surface that generally approximates MSL in the open oceans. Thus, the acquisition of sea-level observations at tide-gauges is the most common method of MSL determination and thence vertical datum definition. MSL observations are affected by three major problems:

1) Sea-level is affected by the presence of tides and other temporal phenomena,
2) The presence of sea surface topography (SST), storm surges, non-linear tides etc. in the coastal zone (Merry and Vaníek, 1983; Pugh, 1987; Hipkin, 2000; Featherstone and Kuhn, 2006);
3) Secular changes in sea level due to climate-related effects (Pugh, 2004).

To determine MSL at a coastal tide-gauge, it is necessary to make sea-level observations over a sufficiently long period to take into account the full tidal signature (Amos, 2007). The major tidal effects (caused by the precession and nutation of the Moon and Sun over an 18.6 year metonic cycle) result in the diurnal (daily) and semi-diurnal (twice-daily) tides that are most noticeable at the coast (Melchior, 1981). Other celestial objects (e.g., planets, etc.) also have effects on the observed tides, but these are much smaller in magnitude than those of the sun and moon (Pugh, 2004).

Chapter 3

3.0 Local Geoids and Existing Global Models

3.1 Introduction

Local or regional geoids pertaining to boundary of interest are mostly accurate within the boundary with increasing distortion as we go beyond the specific region. Each as well may have resulted from different estimation process as there number mechanisms to estimate geoids; Collocation, Stokes' integral, Hotine integral, MSL extrapolation, etc. (see for instance Sansò and Sideris, 2013). They may as well have different accuracies due to the process and the nature of the topography. Notwithstanding the source of data for the computation also gives the level of signals measured for the computation, ground data, airborne, or satellite and among the number of ways data collection is done. Global geopotential models are often computed from satellite data and in some cases ground observations are included, e.g. Satellite-only GOCE model and Satellite with Ground data EGM2008.

3.2 The Italian Quasi-Geoid

The Italian quasi-geoid is computed by Politecnico di Milano. The area covered by the estimate is $35° < lat < 48°$, $5° < lon < 20°$ with grid spacing of 2' both in latitude and in longitude (Barzaghi et al. 2007). The computation is based on remove-restore technique and fast collocation; the solution was obtained in one step only over the whole area. The gravimetric

geoid, integrated with GPS/levelling data has an overall precision of around 3 cm over the entire Italian area.

With regards to the latest Italian quasi-geoid estimation (Italgeo2005), comparing to the previous version of the quasi-geoid, Italgeo9, new data have been taken into account. In particular an up-to-date DTM has been realised on the basis of the NASA SRTM 3" product, integrating it with other national and international data bases. The gravity data base has been significantly integrated and extended in its geographical boundaries. A global geopotential models, based on the space missions CHAMP and GRACE, have been considered, even if the best results have been achieved with the same model used for Italgeo99, i.e. GPM98CR. The quasi-geoid estimation has been computed using the well-known remove-restores procedure. The precision of the estimated gravimetric quasi-geoid, Italgeo2005, has been assessed with the recently updated IGM (Istituto Geografico Militare) GPS/levelling data, attesting an improvement comparing to the previous estimation.

3.3 The Switzerland Quasi Geiod

CHGeo2004Q is the official geoid model used in Switzerland and Liechtenstein. The solution is relative to ETRS89 (GRS80-Ellipsoid) with a resolution of 30". The height reference system is LHN95 (Marti et al. 1998). Compared to the previous version (CHGeo98) a stronger weight was put on gravity and GPS/levelling measurements compared to astro-geodetic data and a global model (EGM96) was used as a reference. The model CHGeo2004Q is sold for commercial use but can be made available for free for pure scientific purposes. The deviation from the local reference ellipsoid in Switzerland reaches amounts up to ±5 m. The geoid model in Switzerland (CHGeo2004) was determined from a combination of all methods and shows an accuracy of 1 to

3 cm. The Swiss geoid model is available in the form of a 1-km grid and can be integrated in practically all of the commercially available GPS receivers.

3.3 The French Quasi Geoid

A header (unit degree) southern latitude northern latitude western longitude eastern longitude latitude increment longitude increment- quasi-geoid undulation in meters from north to south and for each latitude from west to east (Duquenne et al. 1997).

3.4 The European Quasi Geoid

The EGG97 geoid and quasigeoid data are of resolution 10m x 15m and 10m x 15m, respectively. The grid spacing of these files is 10' x 15'. The full resolution files (1.0' x 1.5') are not available as public domain data and must be obtained through the IAG Secretary General (http://www.gfy.ku.dk/~iag/egg97.html) (Denker et al. 1997). The model is based on gravimetric data both land and airborne. The grid values are given in rows from West to East. The rows are given from North to South. Thus, the first data value refers to the NW corner of the grid, and the last data value refers to the SE corner of the grid. The grid values are given in mm. The values refer to GRS80 ellipsoid and the zero tide system (as recommended by IAG).

Country	Max (m)	Min (m)	Mean (m)	Standard Deviation (m)
Italy_QG	0.28	-1.65	-0.21	0.40
Swiss_QG	0.35	-1.27	-0.06	0.22
French_QG	-0.04	-1.78	-0.28	0.56
European_QG	0.74	-2.15	-0.18	0.36

Table 3.1: Quasigeoid data minus GOCE and EGM2008 used in the computations

3.5 The Satellite Only GOCE Model

The satellite only Gravity field and steady-state Ocean Circulation Explorer (GOCE) models were computed in three different ways (Pail et al. 2011), parameterizing them in terms of spherical harmonic coefficients, from 71 days acquired data. The three computation procedures are the Direct approach (DIR), The Time-wise approach (TIM) and The Space-wise approach (SPW). The three approaches, which are based on different and complementary processing philosophies. The direct approach (DIR) and the time-wise approach (TIM) assemble and solve large normal equation systems to estimate the harmonic coefficients as parameters. While DIR starts with an a priori gravity field model and adds GOCE information to improve it, the rationale of TIM is to compute a GOCE-only model in a rigorous sense, which is solely based on GOCE data. In contrast, SPW works predominantly in the space domain, applying least squares collocation and exploiting spatial correlations of the gravity field GOCE provides significant additional information of the global Earth gravity field, with an accuracy of the 2-month GOCE gravity field models of 10 cm in terms of geoid heights, and 3 mGal in terms of gravity anomalies, globally at a resolution of 100 km (degree/order 200) (Reguzzoni, 2010). In this way, data which are close in space but far in time can be filtered together, thus overcoming the problems related to the strong time correlation of the observation noise (Reguzzoni, 2010). The GOCE target was to have the knowledge of the static gravitational potential; hence corrections were applied to the observation equations in order to remove time varying effects like luni-solar attraction, tides and non-tidal effects.

The functional model representing the anomalous potential V(r, ϑ, λ) in spherical coordinates (with radius r, co-latitude ϑ, longitude λ) in spherical harmonics is a series of spherical harmonics truncated at maximum degree N:

$$V(r,\vartheta,\lambda) = \frac{GM}{a}\sum_{n=2}^{N}\ \sum_{m=-n}^{n} A_{nm}\left(\frac{a}{r}\right)^{n+1} Y_{nm}(\vartheta,\lambda) \qquad (3.1)$$

Where G is the gravitational constant, M mass of the Earth, a equatorial radius of the Earth ellipsoid and Y_{nm} surface spherical harmonics of degree n and order m

$$Y_{nm}(\vartheta,\lambda) = \bar{P}_{n|m|}(\vartheta,\lambda)\begin{cases}\cos m\lambda & m \geq 0\\ \sin|m|\lambda & m < 0\end{cases}$$

$\bar{P}_{n|m|}(\vartheta,\lambda)$ are the fully normalized associate Legendre functions, and $A_{nm} = C_{\mathbf{nm}}$, $S_{n|m|}$ are the spherical harmonics coefficients to be determined, with C_{nm} for $m \geq 0$, and $S_{n|m|}$ for $m < 0$.

The space-wise GOCE model is estimated from both the satellite tracking data derived from the on board GPS receiver and a gravity gradients observed by the on board electrostatic gradiometer.

GOCE is better that GRACE from degree 70 to 120 and beyond. Extending to degrees higher 180, EGM2008, the quality of the EGM2008 model is superior; hence the differences between them are true representation of the true error. The maximum degree of the GOCE space-wise solution is chosen equal to 210 with a commission error of the order of 10 cm, where the error degree variances reach the signal degree variances, before being strongly regularized (Reguzzoni, 2010).

3.6 The Earth Gravitational Model 2008 – EGM08

EGM2008 is a spherical harmonic model of the Earth's gravitational potential, developed by a least squares combination of the ITG-GRACE03S gravitational model and its associated error covariance matrix of degree and order 180, with the gravitational information obtained from a global set of area-mean free-air gravity anomalies defined on a 5 arc-minute equiangular grid. This global set of gravity anomalies was formed by merging terrestrial and airborne data with altimetry-derived values. Over certain areas where the available gravity anomaly data could only be used at a lower resolution, their spectral content was supplemented with the gravitational information obtained from a detailed global topographic database. EGM2008 is complete to degree and order 2159, and contains additional coefficients up to degree 2190 and order 2159. Over areas covered with high quality gravity data, the discrepancies between EGM2008 geoid undulations and independent GPS/Levelling values are on the order of ±5 to ±10 cm.

The data for the high resolution global gravitational model 2008, are GRACE data, accompanied by its complete error covariance matrix, a complete global set of 5 arc-minute area-mean free-air gravity anomalies and high resolution global Digital Topographic Model (DTM).With least squares estimation procedure, EGM2008 has been developed by an iterative procedure as follows (Palvis,2008):

- Step 1: A Mean Sea Surface (MSS) and a GRACE-only gravitational model are used to derive a low degree and order spherical harmonic expansion of the DOT (Dynamic Ocean Topography).

- Step 2: Satellite altimeter data, along with the estimated DOT model, are used to estimate an ocean-wide set of free-air gravity anomalies.
- Step 3: The altimetry-derived free-air gravity anomalies are merged with corresponding values over land, and are supplemented with some "fill-in" values over areas void of any gravity observations, to form a complete global 5 arc-minute equiangular grid of surface free-air gravity anomalies.
- Step 4: The 5 arc-minute surface free-air gravity anomalies are continued analytically to the surface of an ellipsoid of revolution.
- Step 5: The 5 arc-minute free-air gravity anomalies on the ellipsoid and their associated error estimates are input to a Block-Diagonal (BD) least squares estimator, which produces a "terrestrial" estimate of the gravitational potential coefficients, accompanied by a set of BD normal equations. The fact that a spherical harmonic expansion of the gravitational potential complete to degree and order 2159 involves approximately 4.7 million coefficients is what necessitates here the BD approximation of the normal equations.
- Step 6: The GRACE-only normal equations' matrix is approximated so that it adheres to the same BD pattern that was used in the "terrestrial" gravity normal equations, by simply equating to zero the elements of the matrix that reside outside the diagonal blocks of interest. The two sets of BD normal equations are then combined and inverted to yield the potential coefficients of the combination solution and their associated error estimates.
- Step 7: The MSS from Step 1 and the combination solution from Step 6 are used to estimate a new model of the DOT. Using this new DOT model, one returns to Step 2 and re-iterates the process.

The development of EGM2008 is based on Molodensky's theory, which determines the external gravity filed of the Earth without any assumptions concerning the density of the masses above the geoid (Heiskanen and Moritz, 1967), (Pavlis, 2008). The Earth's external gravitational potential, V, at a point P defined by its geocentric distance (r), geocentric co-latitude (θ) (defined as 90°-latitude), and longitude (λ), is given by:

$$V(r,\theta,\lambda) = \frac{GM}{r}\left[1 + \sum_{n=2}^{\infty}\left(\frac{a}{r}\right)^{n}\sum_{m=-n}^{n}\bar{C}_{nm}^{s}\bar{Y}_{nm}(\theta,\lambda)\right] \quad (3.2)$$

where GM is the geocentric gravitational constant and a is a scaling factor associated with the fully-normalized, unit less, spherical harmonic coefficients $\bar{C}_{nm}^{s}$. The superscript "s" identifies the coefficients as being spherical. a is usually numerically equal to the equatorial radius of an adopted reference ellipsoid. The above Equation refers to the permanent part of the gravity field, either ignoring or having corrected first for the variable part due to tides, changes in Earth rotation, etc. (Pavlis, 2008). The fully-normalized surface spherical harmonic functions are defined as in Heiskanen and Moritz (1967):

$$\bar{Y}_{nm}(\theta,\lambda) = \bar{P}_{n|m|}(\cos\theta)\begin{cases}\cos m\lambda & if\ m \geq 0\\ \sin|m|\lambda & if\ m < 0\end{cases}$$

$\bar{P}_{n|m|}(\cos\theta)$ is the fully-normalized associated Legendre function of the first kind, of degree n and order m. The disturbing potential T as the difference between the actual gravity potential of the Earth and the "normal" gravity potential associated with a rotating equipotential ellipsoid of revolution expressed in the WGS 84 Geodetic Reference System. Provided that the rotational speed of the reference ellipsoid is the same as the actual rotational speed of the Earth, so that

actual and normal centrifugal potentials would cancel out, the spherical harmonic expansion of Tis given by (Pelvis, 2008):

$$T(r,\theta,\lambda) = \frac{GM}{r}\left[\sum_{n=2}^{\infty}\left(\frac{a}{r}\right)^{n}\sum_{m=-n}^{n}\bar{C}_{nm}^{s}\bar{Y}_{nm}(\theta,\lambda)\right]$$

The zero degree term of the above equation is set to zero, forcing the equality of the actual mass of the Earth and the mass of the reference ellipsoid (Pavlis, 2008).

The least square estimation solution represents an estimate of the ellipsoidal harmonic gravitational potential coefficients, which was obtained solely on the basis of the "terrestrial" gravity anomaly data. These data suffer from significant long wavelength errors. In contrast, the gravitational information obtained from satellite tracking data is highly accurate at long wavelengths, but lacks short wavelength details, due to the attenuation of the gravitational signal with altitude (Pavlis, 2008), hence the complementary characteristics of terrestrial and satellite data was employed in the modelling of EGM2008 unlike satellite only GOCE to work well at both low and high frequencies. EGM2008 is therefore a combine solution of the satellite-only information and the gravity anomaly data from degree 2 to 2159. The satellite data is up to a relatively low degree, maximum of the satellite-only solution and beyond this degree, the area-mean gravity anomaly data is used.

The least squares adjustment combination was performed in terms of ellipsoidal harmonics. The combined solution and its error estimates were then converted to spherical harmonics. This conversion preserves the order but not the degree, thus giving rise to model coefficients extending to degree 2190 and order 2159. The fact that the normal equations of ITG-GRACE03S

are predominately block-diagonal permitted the combination solution to be performed in a very efficient way, without compromising the accuracy of the results (Pavlis, 2008).

3.7 The Hypothesis of GOCE (0-200) + EGM2008 (201-900)

The estimation of the long and short wavelength of the local geoid can be well catered for by GOCE and EGM2008. The satellite-only GOCE model is able to give (and therefore remove) the medium long wavelength without biases up to degree and order 180 (corresponding to a spatial resolution of about 100km).

If necessary the high frequency can be removed from local models using EGM08. In fact it is well known that high frequencies are very little influenced by biases (see. Gatti et al. 2013).

Chapter 4

4.0 Data Processing and Geoid Alignment

4.1 Region of estimation

The final geoid model is expected to be continuous also at the boundaries of the countries meeting the in the study region. The considered area extends from latitude 42^{o}N to 48^{o} N and Longitude 4^{o}E to 15^{o}E (see figure 4.1) and include the quasi-geoids of Italy, France, Switzerland. The European Quasi-Geoid was use to fill part of Germany, Austria, Slovenia, Mediterranean Sea (see figure 4.2).

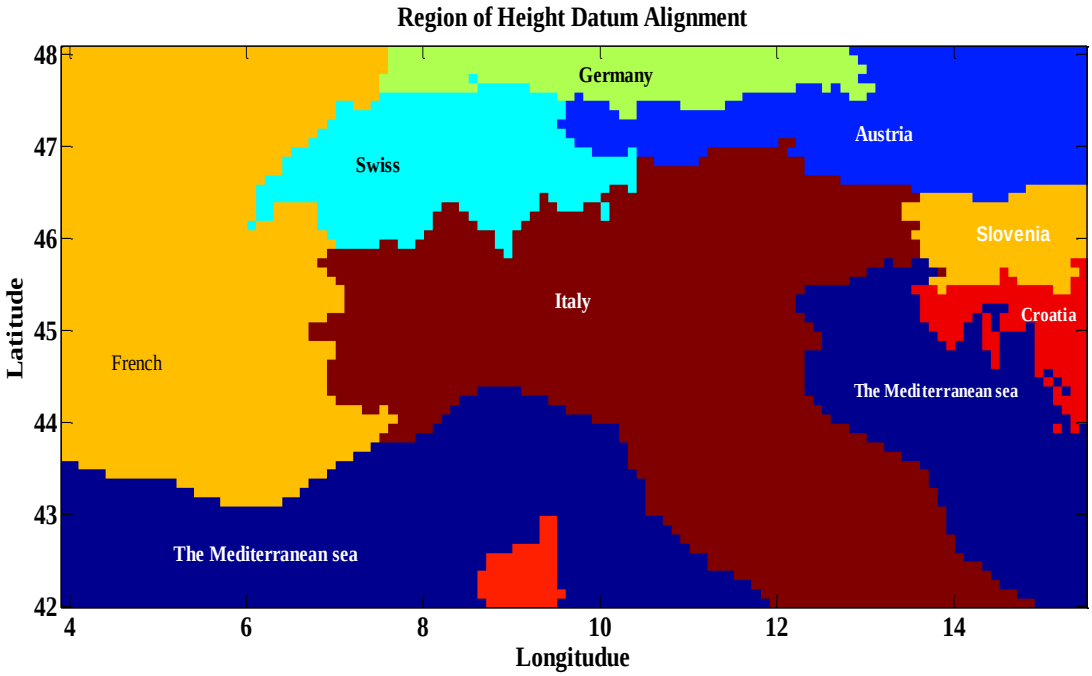

Figure 4.1: Area for height datum alignment

Aligning these height datums is done by finding the best approach to takeout the individual bias and thereafter by merging the boarders. As for the latter problem, i.e. the geoid merging at the boundaries, different solutions (namely least square approach, Kriging or collocation) has been implemented. The estimation principle of the bias requires the best fit for individual geoid which can be a constant or the four parameters (i.e. a constant and three translation parameters).

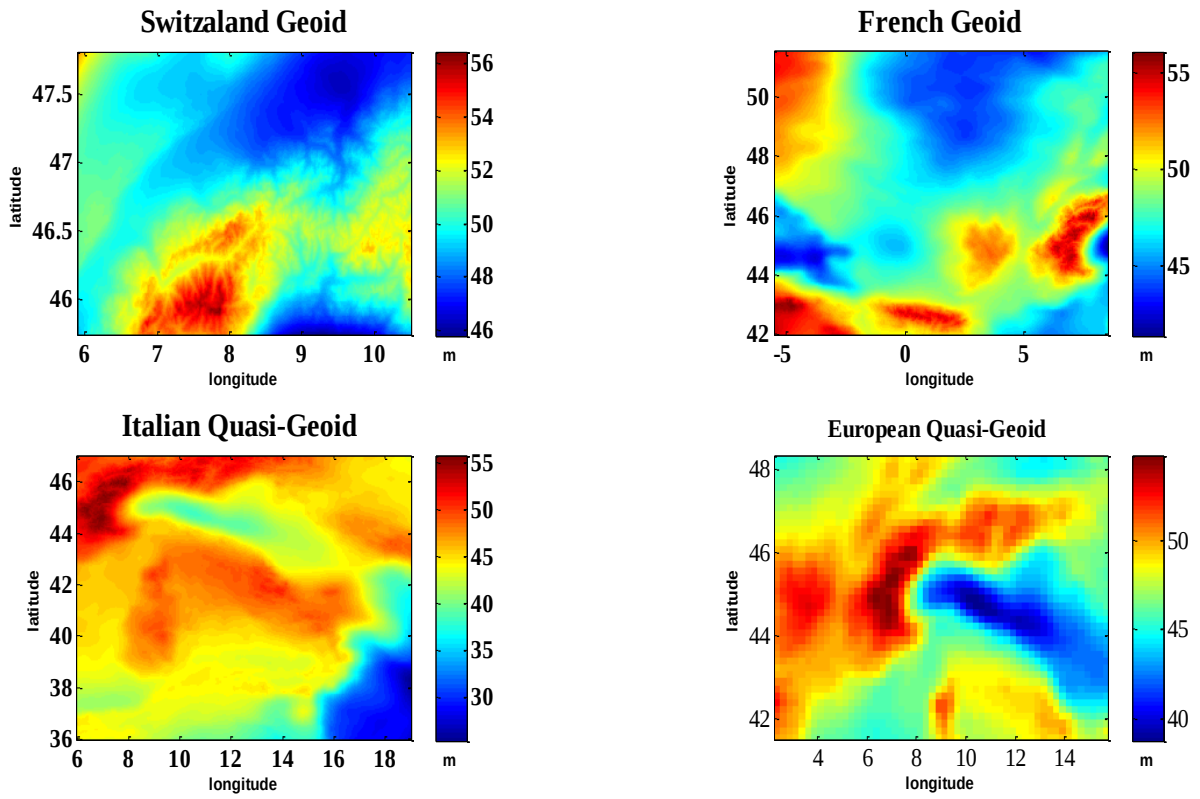

Figure 4.2: The Quasigeoids for the study area; Swiss, Italy, French and part of Eastern Europe

4.2 Data Processing

Each quasigeoid for the height datum alignment has different resolutions and accuracies. The Switzerland geoid has the best resolution 30'' and the Italian geoid 2', the French 1' and the

worst among them being the European geoid 10'x15'. A new grid with a spatial resolution of 3'x3' is created and it is used to interpolate the geoids on the same points in the computation region. The interpolation mechanism employed is a linear interpolation of the geoid undulation N for every couple of latitude φ and longitude λ on the new grid. This results in either improving or worsening the resolution of the composing quasi-geoids. Notwithstanding the linear interpolation procedure also affects the undulation in some regions, mostly at the Alps areas, but this was not investigated which can be future work on the best function for interpolation around the Alps.

The interpolation was done separately, from each geoid to the 3'x3' grid mask and the data bounded within individual countries were put together. The new geoid model depicts boundary jumps at the meeting boarders. Some were very distinct which can be a number of reasons; the various reference ellipsoid used in computing each quasigeoid model, the accuracy of each geoid interpolated, the varying effects of the interpolation mechanisms at some points, the different resolutions of the original data. The four maps are shown in figure 4.3 while the interpolated geoid is shown in figure 4.4 and a 3D perspective in figure 4.5. The discontinuities at the boundaries are enhanced in figure 4.6 by differentiating in the latitude direction as the plot the deflection of the vertical.

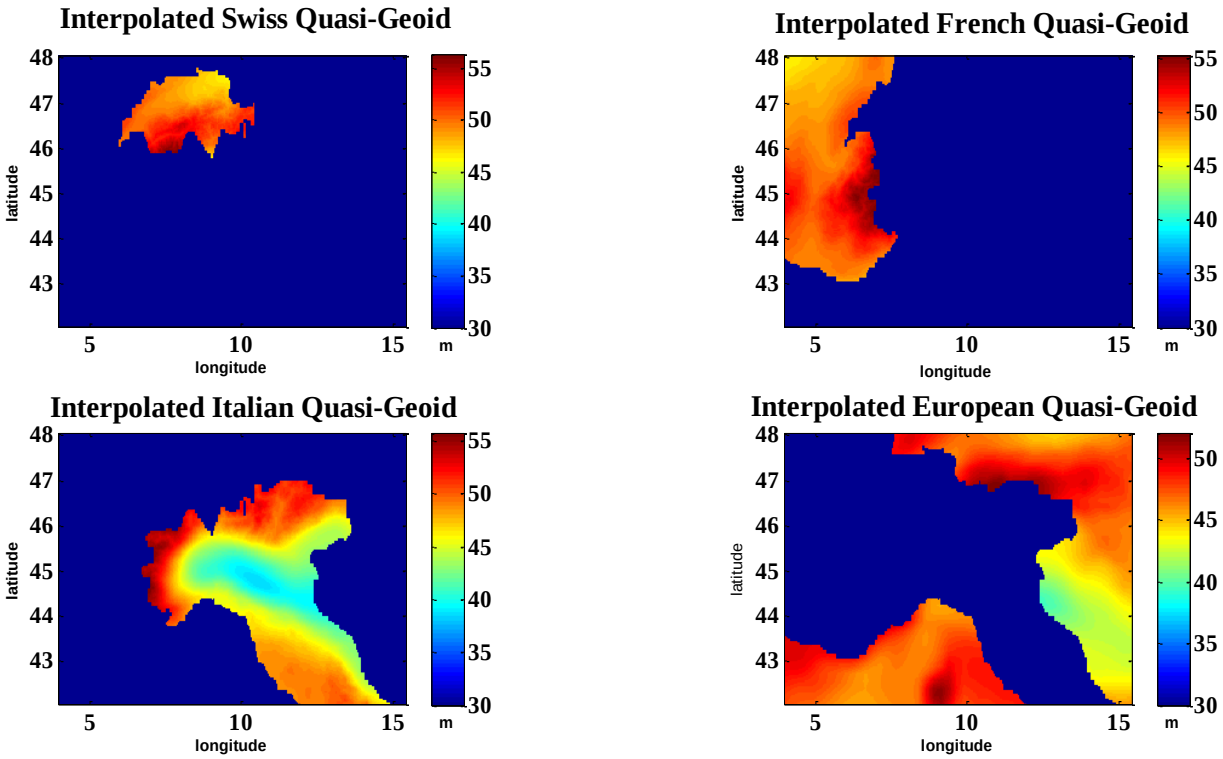

Figure 4.3: Quasigeoid within borders of respective countries

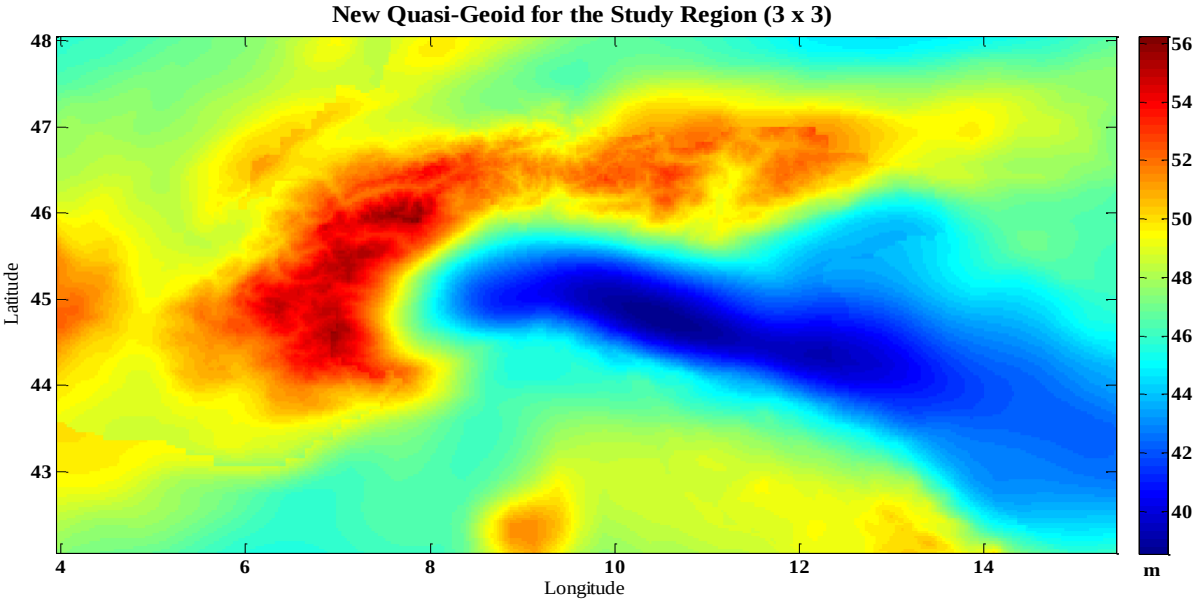

Figure 4.4: The four merge models showing boundary discontinuities

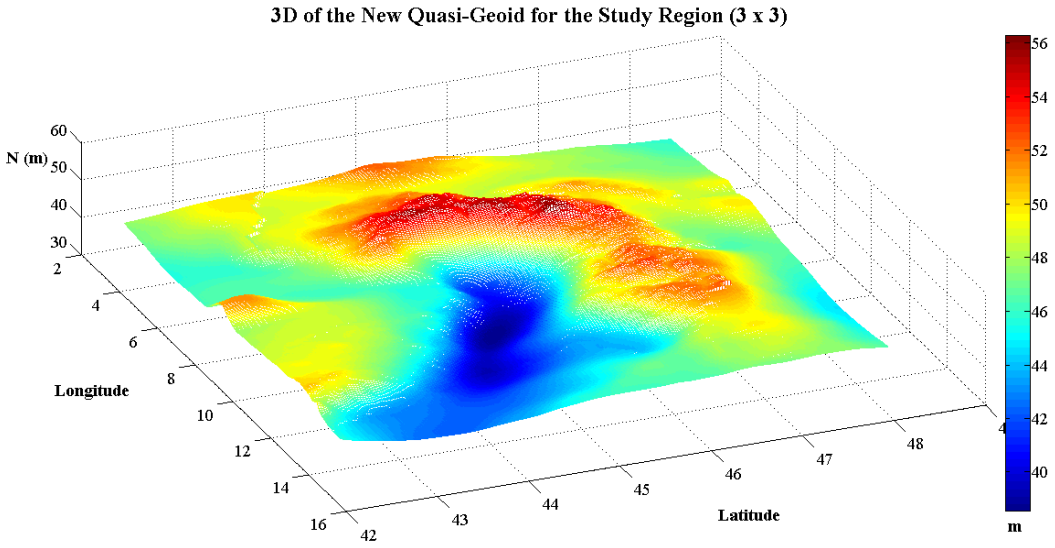

Figure 4.5: 3D perspective of the four merges models showing boundary discontinuities

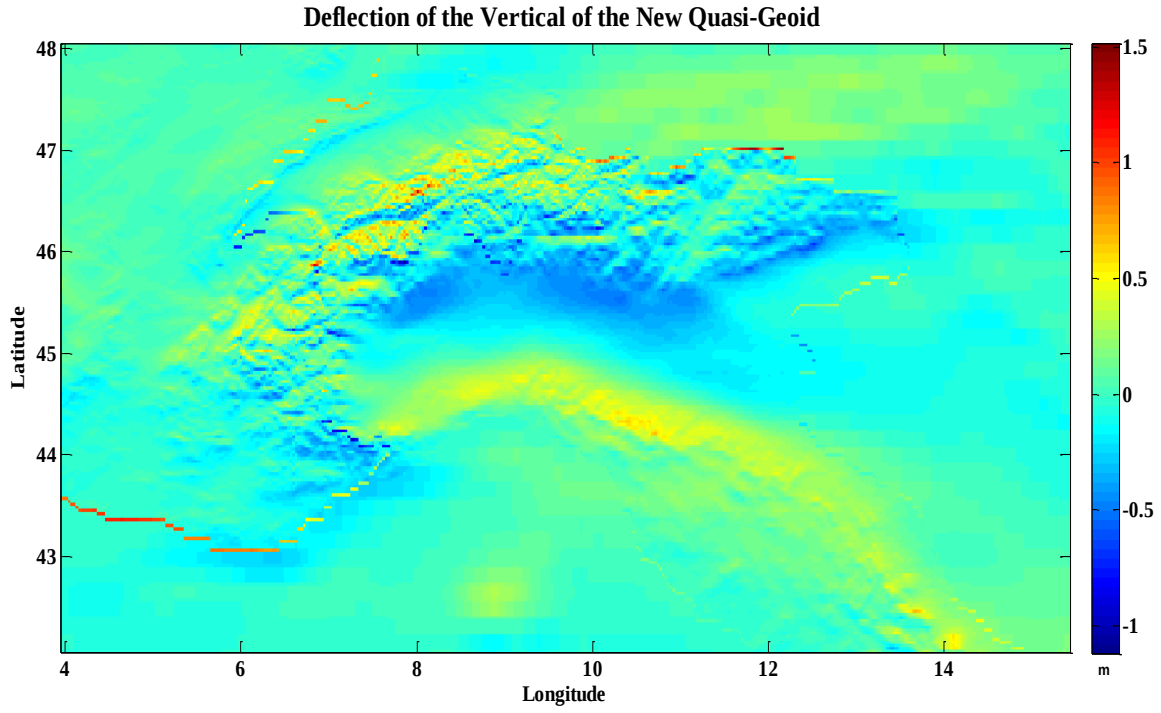

Figure 4.6: Deflection of the vertical of the geoid model showing border effects

4.3 The Model Alignment

Computing the stochastic and deterministic part of the new model requires some assumptions in choosing the frequencies as well as the translation parameters. In the modelling process, the low frequencies from zero to 200 and the high frequencies from 201 to 2159 were considered deterministic, as well as the bias as in the formula below:

$$N_r = \underbrace{N - N_L - N_H + b(\varphi, \lambda)} + \upsilon$$

deterministic part

Where N_r is the residual signal computed by removing from the local geoid N the low frequency N_L and the high frequencies N_H. This residual is considered as the sum of the unknown bias model $b(\varphi, \lambda)$, that can be model for instance by a constant or by a function of φ and λ, and the stochastic model υ which is the error part, i.e. the sum of the errors of each local geoid υ_L and the errors of the global models υ_{GM}.

$$\upsilon = \upsilon_L + \upsilon_{GM}$$

The computation of the low frequencies from 0 – 200 was done using GOCE (figure 4.7). GOCE is superior at low frequencies compare to EGM2008. Using spherical harmonic manipulator (Andrea Gatti, et al 2013), frequencies from zero to 200 was computed, inputting the parameters, φ and λ and radius at each point. The harmonic manipulator converts the geodetic reference system to geocentric reference system for the computation. GOCE was examined for different frequencies combinations (0-120, 0-180, 0-200) to see best takes care of the low frequencies. The table below (table 4.1) shows the minimum and maximum for the residuals after removing each frequency combination.

Frequencies of GOCE model	Min of residual (m)	Max of residual (m)	Mean (m)
0 – 120	-7.03	4.43	-0.77
0 – 180	-6.40	4.83	-0.72
0 – 200	-3.91	3.06	-0.74

Table 4.1: Range of the high frequencies residual range after removing GOCE to some degrees

In the harmonic manipulator, the anomalous potential T is computed and then used in the relation $N = T/\gamma$, where γ is the normal gravity to the reference ellipsoid.

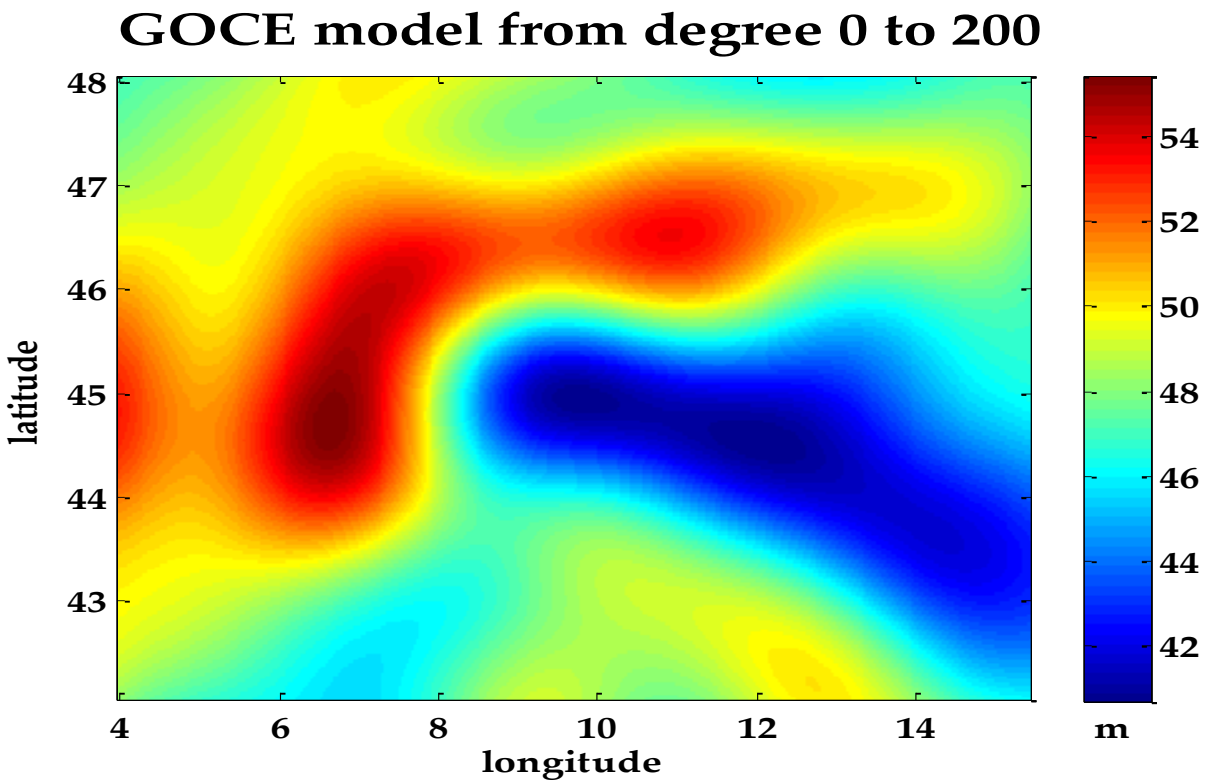

Figure: 4.7 Estimate from GOCE model up to degree 200 of the study region

The resulting residual after removing the low frequency part with GOCE up to degree 200 (figure 4.8) is in the range of -4 to 3 meters. The effect of the patched geoid obtained by merging the local models can be clearly seen in figure 4.8, e.g. in correspondence of the boundary between France and the Mediterranean Sea or between Italy and Austria.

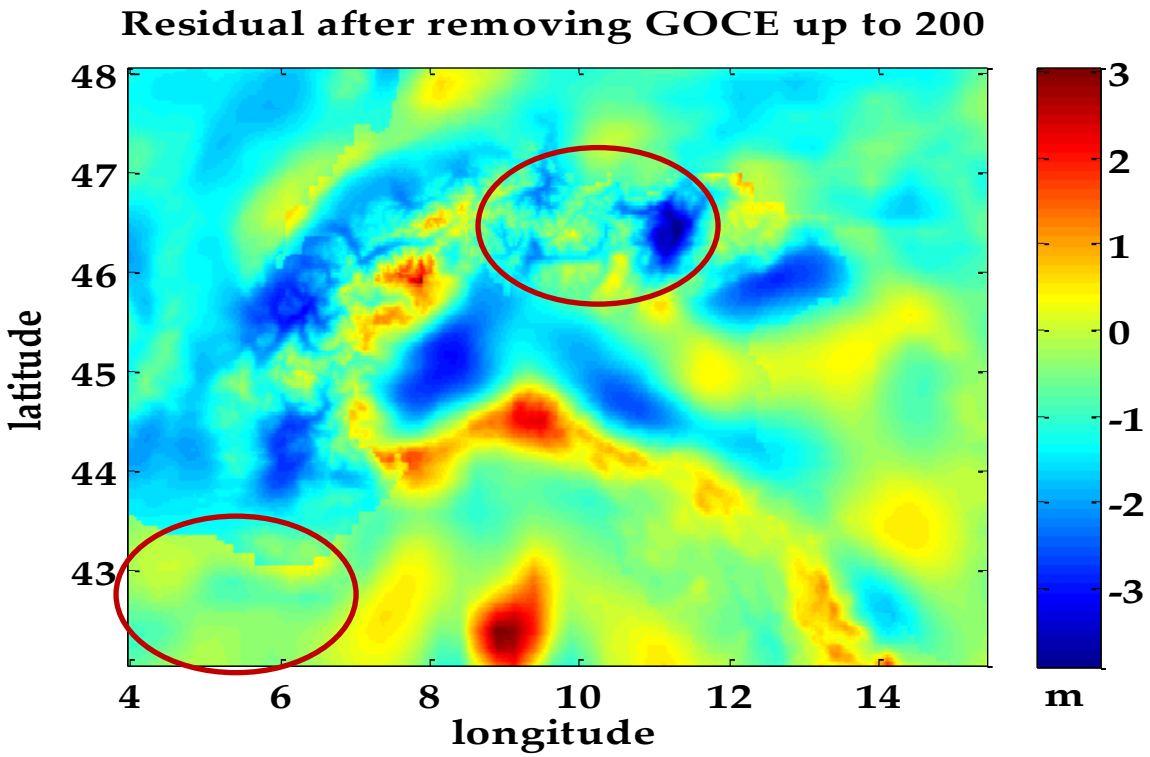

Figure 4.8: Residuals after removing GOCE up to degree 200

The next step is to remove the high frequencies from degree 201 to 2159 with the EGM2008 model (figure 4.9), which is good at high frequencies. The errors of both models are still present in the residual with the local geoid errors. Figure 4.10 shows the final residuals after removing the high frequency part using the spherical harmonics manipulator.

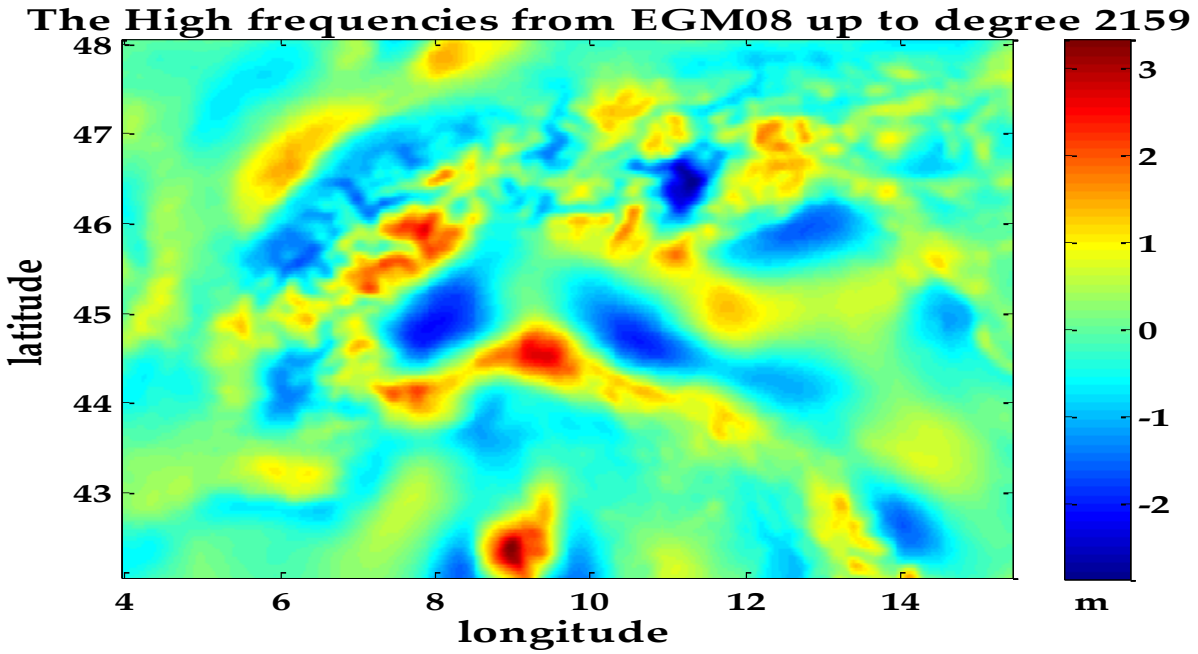

Figure: 4.9: Synthesis of the high frequencies from EGM2008 model from degree 201 to 2159

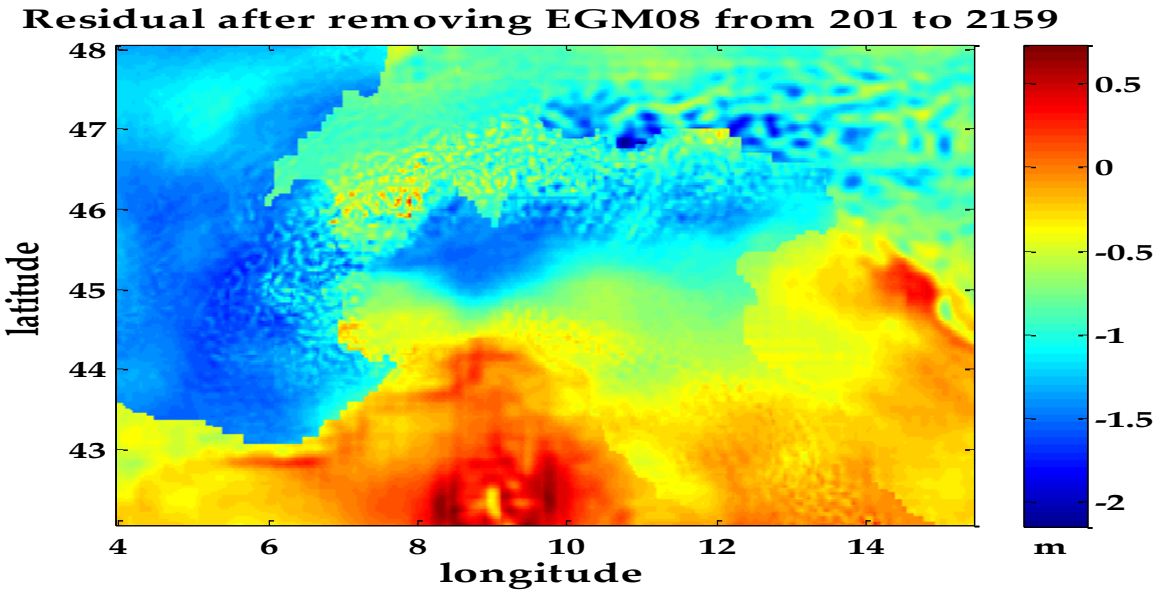

Fig: 4.10. The very high Frequencies showing border effects after removing EGM2008 (2159)

The border effects are very much obvious after removing GOCE and EGM08. The residuals are in the range of -2 to 0.7 meters. This is mainly due to the different height datums used, showing the local biases in each local geoid. The effects of the different accuracies and the spatial resolutions are also contributing factors to the jumps at the borders. The Computations resulting in the residuals with the border effect was estimated from the relation:

$$Residual_{(biased)} = N - GOCE_{(0-200)} - EGM08_{(201-2159)} \quad (4.2)$$

4.4 Least Square estimation of the Biases

The estimation of the respective bias is very critical due to the varying source of the biases in each quasigeoid. Notwithstanding, the geometry of the individual models also poses a challenge in choosing a unique approach that can correct all the biases in the quasi-geoids at one solution. There is therefore the need to investigate which estimation approach that fits all with little or no jumps, either a constant or a constant with a linear trend.

4.4.1 Linear Trend Bias – Four Parameters for each Quasigeoid

The systematic effects are estimated using least squares procedure, with a co-factor matrix comprising of the errors of the global models GOCE and EGM08 and errors of the local geoids. A constant bias or a constant with a trend were computed for each country to see which best remove the border effects. From the block covariance of GOCE the variance - covariance for the observations and with neighbouring countries were computed for the stochastic part of GOCE. Likewise the same estimation was done fromEGM08 using the standard deviation (degree variance) since the block covariance is not available. Errors of the individual local geoids were

assumed as white noise, which is rather a strong assumption for gravity observations. The function below shows the total covariance for the estimation of the biases.

$$Q_{error} = \left[C_{(GOCE)}\right] + \left[C_{(EGM08)}\right] + \left[C_{(vv)}\right] \tag{4.3}$$

$$C_{GM}(r, r', \psi) = \left(\frac{GM}{a}\right)^2 \sum_n \sigma_n^2 \left(\frac{a^2}{rr'}\right)^{n+1} P_n(\cos\psi) \tag{4.4}$$

The error covariance matrix structure Global models is computed from Eq. (4.4), while the white noise identity matrix C_{vv} comes from corresponding errors of each geoid. The design matrix for the computation has for the constant bias estimates one parameter for each geoid, while the trend bias gives four parameters. Due to the large data size, a matrix of 200 x 383 giving total observations of 76600, making computation of the covariance and inverting the matrix not feasible, the data was down sampled to 8576. This will not affect the estimation of the parameters, as four parameters are estimated for each Geiod when considering a linear trend with a constant and a single parameter when considering a constant for each geoid. In the linear trend estimation the observation equation of the four parameters is given by:

$$B_i = a_i + b_i \cos\Phi \cos\lambda + c_i \cos\Phi \sin\lambda + d_i \sin\Phi + v_i \tag{4.5}$$

Where a_i is the origin of the geoids and b_i, c_i, d_i, is the translation of the barycentre and *i* for each geoid. Therefore the design matrix for the estimation is given as for *i* = 1, 2, 3, 4,

$$\Delta = \underset{\text{m x 16}}{\begin{bmatrix} B_{it} & \emptyset & \emptyset & \emptyset \\ \emptyset & B_{ch} & \emptyset & \emptyset \\ \emptyset & \emptyset & B_{fr} & \emptyset \\ \emptyset & \emptyset & \emptyset & B_{eu} \end{bmatrix}} \qquad X = \underset{\text{16 x 1}}{\begin{bmatrix} a_i \\ b_i \\ c_i \\ d_i \end{bmatrix}} \qquad Q_{error} = \underset{\text{m x m}}{\begin{bmatrix} \sigma^2 & \cdots & c(\psi) \\ \vdots & \ddots & \vdots \\ c(\psi) & \cdots & \sigma^2 \end{bmatrix}} \tag{4.6}$$

The observation, herein being the residuals after removing the low and high frequencies is a column vector of m observations.

$$r = \begin{bmatrix} \delta N_{iti} \\ \vdots \\ \delta N_{chi} \\ \vdots \\ \delta N_{fri} \\ \vdots \\ \delta N_{eui} \\ \vdots \\ \delta N_{eum} \end{bmatrix} \quad \text{m x 1}$$

From least squares the parameters x is given by $x = \left(\Delta^t * Q^{-1}{}_{er} * \Delta\right)^{-1} * \left(\Delta^{-1} * Q^{-1}{}_{er} * r\right)$

The significance of the estimated parameters cannot be analysed independently, but applying to the observation matrix the shape of the bias can be constructed and the figures 4.11 and 4.12 show the bias for each country and the merged bias. Comparing the residuals with the biases, it can be inferred that the linear trend fits well the Italian and European quasi-geoids than the French and Switzerland.

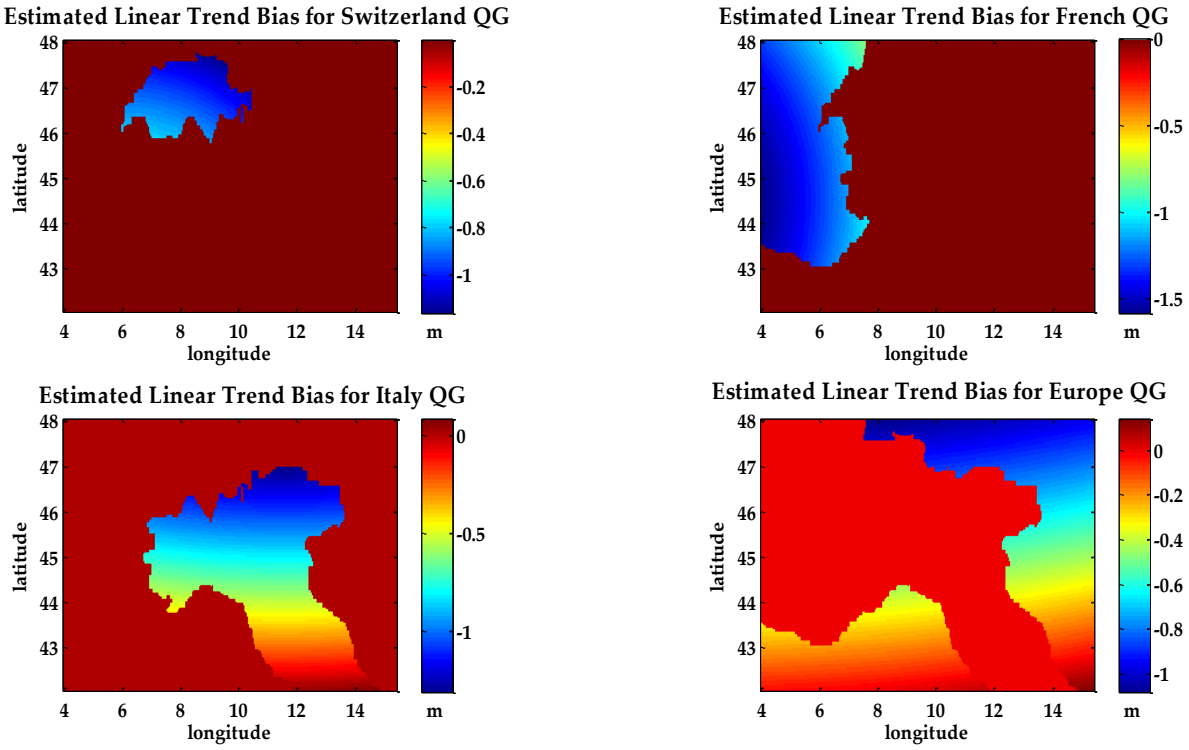

Figure 4.11: The Estimated trend biases from the parameters

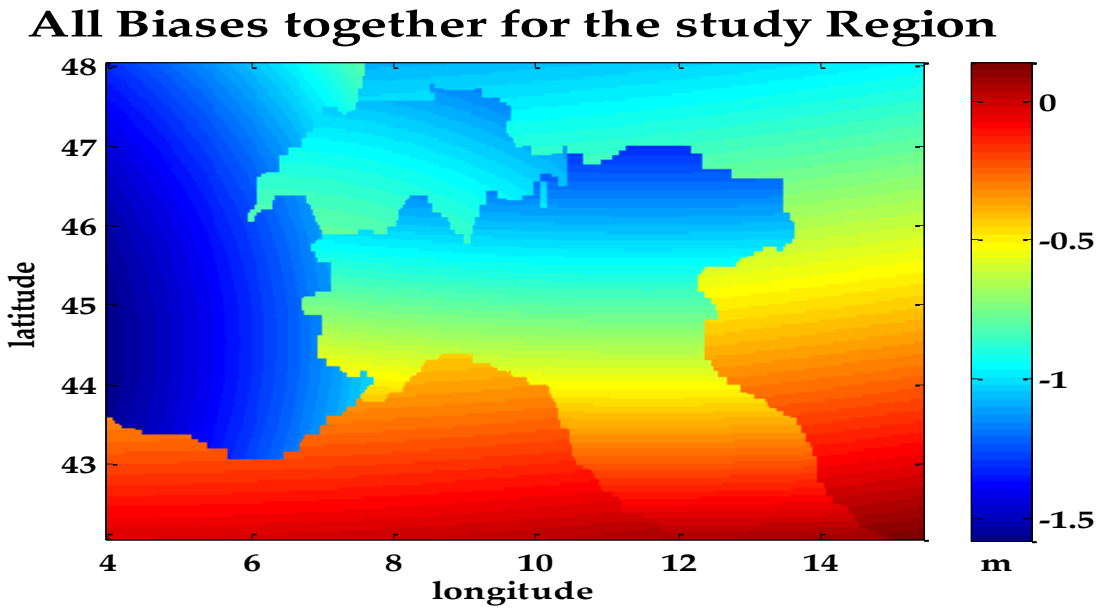

Fig: 4.12: Merged bias

This computation determines for each quasigeoid a constant with a trend different from the neighbouring geoid model. Here it is evident, the jumps also in the biases at the borders when put together figure 4.12. The biases were applied to the residuals after GOCE and EGM08 to correct the border effects, figure 4.13. It is expected that there will be no significant jumps at borders, and if there exist any, the order of magnitude should be in millimetres. This is not the case with European quasi-geoid, it can be seen that the borders sheared among Italy, France and Switzerland were better corrected and jumps are within millimetre level but not with boundaries sheared with the European quasi-geoid. Here the jumps are within the order 0.80 to 1.2 meter close to the Alps and about 0.40 meters at the Mediterranean Sea region. This can be attributed to the low spatial resolution of the European quasigeoid used.

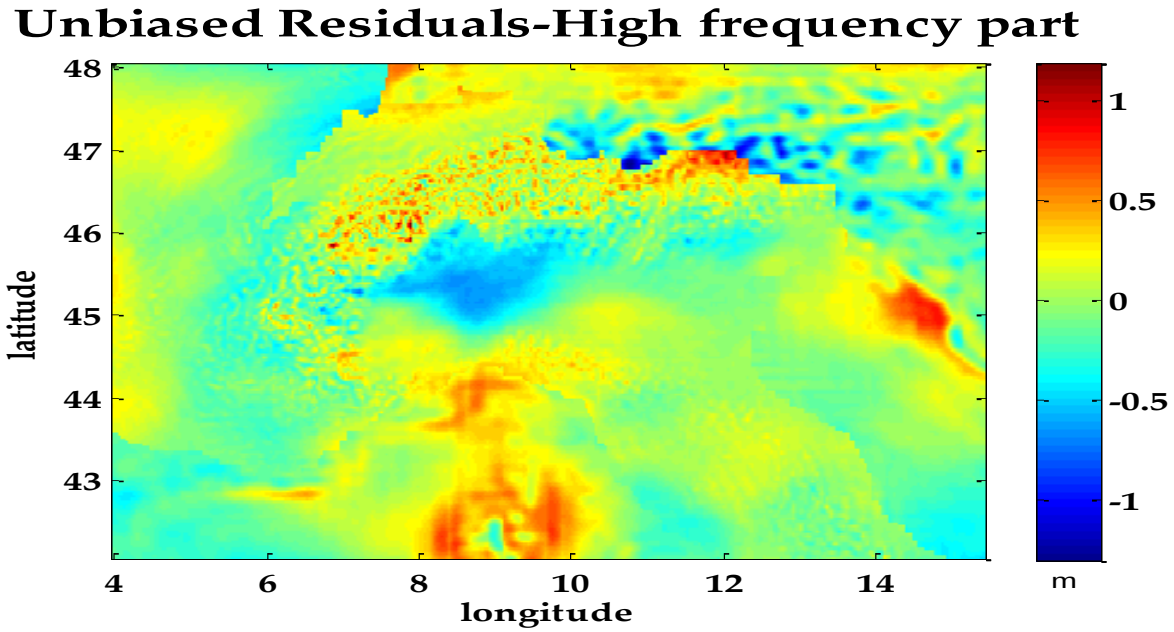

Figure 4.13: Unbiased residuals (very high frequencies of the signal)

The statistics of the residuals are presented in the table 2.3. After the bias the residuals should have close to zero mean, shown in figure 2.4 is the probability distribution plot of the residuals with a Gaussian curve fit. The plot fit a normal distribution curve.

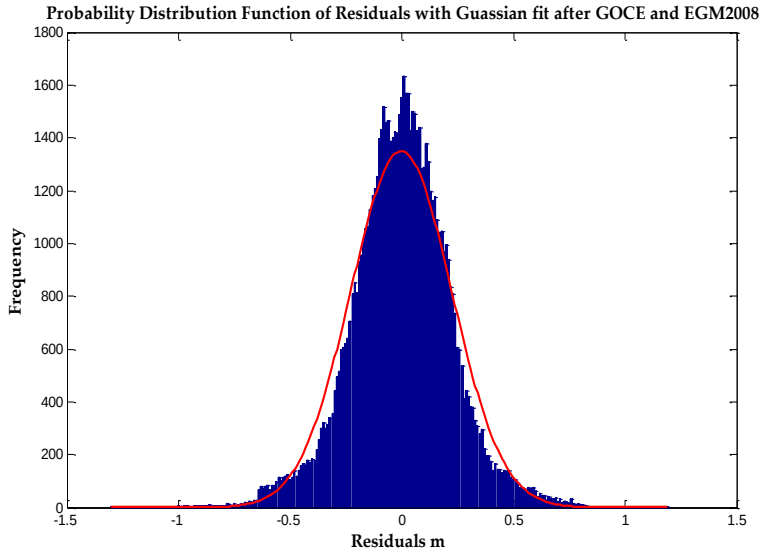

Fig: 4.14 Probability Distribution Function of the residuals

max	119 cm
min	-130 cm
Mean	0.25 cm
STD	22.61 cm
Variance	5.1 cm

Table 4.2 Stat of Residuals

4.4.2 The Constant Bias

Another approach was to see how best the biases can correct the border effects if constant bias is estimated for each quasigeoid. The approach is not different from the case of a trend. Here the equations are modified by taking out the parameters of the translation of the barycentre b_i, c_i, d_i.

$$B_i = a_i + v_i \tag{4.7}$$

Where a_i is the origin of the geoids, therefore the design matrix for the estimation is given as for i = 1, 2, 3, 4,

$$\Delta = \underset{m \times 4}{\begin{bmatrix} B_{it} & \emptyset & \emptyset & \emptyset \\ \emptyset & B_{ch} & \emptyset & \emptyset \\ \emptyset & \emptyset & B_{fr} & \emptyset \\ \emptyset & \emptyset & \emptyset & B_{eu} \end{bmatrix}} \qquad X = \underset{4 \times 1}{\begin{bmatrix} a_i \\ b_i \\ c_i \\ d_i \end{bmatrix}} \qquad Q_{error} = \underset{m \times m}{\begin{bmatrix} \sigma^2 & \cdots & c(\psi) \\ \vdots & \ddots & \vdots \\ c(\psi) & \cdots & \sigma^2 \end{bmatrix}} \tag{4.8}$$

The observation r, herein being the residuals after removing the low and high frequencies is a column vector of m observations.

$$r = \underset{m \times 1}{\begin{bmatrix} \delta N_{iti} \\ \vdots \\ \delta N_{chi} \\ \vdots \\ \delta N_{fri} \\ \vdots \\ \delta N_{eui} \\ \vdots \\ \delta N_{eum} \end{bmatrix}}$$

From least squares the parameters x is given by $x = \left(\Delta^t * {Q^{-1}}_{er} * \Delta\right)^{-1} * \left(\Delta^{-1} * {Q^{-1}}_{er} * r\right)$

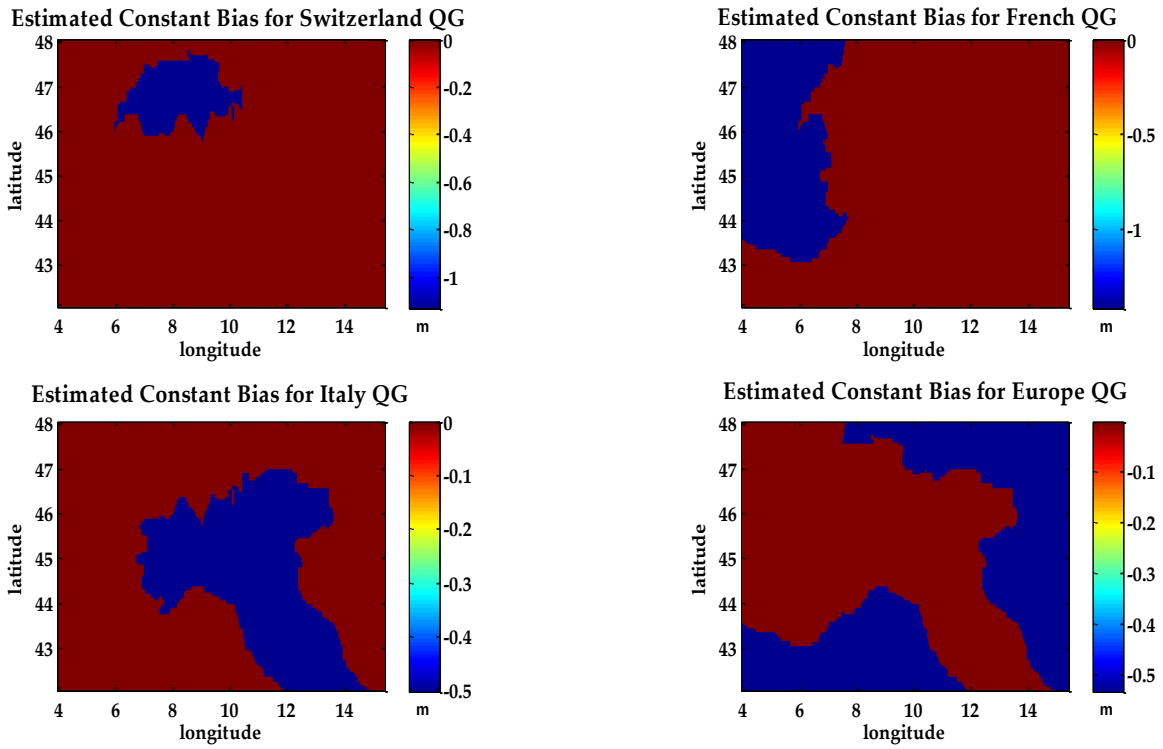

Figure 4.15: The Estimated constant biases from each parameter

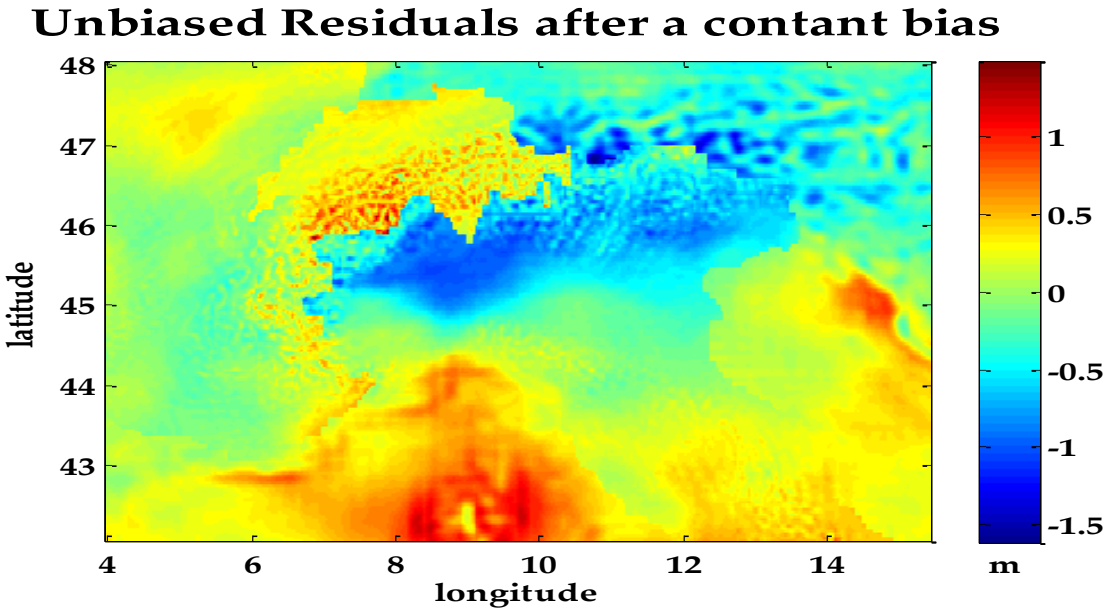

Figure 4.16: unbiased residuals (very high frequencies of the signal)

Comparing the statistics of the constant bias remove with the linear trend removal, it is seen that the systematic effects are better solved by linear trend (four parameter estimation of bias). Even though the four parameters linear trend approach did not completely align the geoids at the borders and there are significant jumps showing. The probability distribution plot of the residuals after the constant biases is right skewed, which proves that there is still a sizable bias present in the residuals. Quasi-geoids of Italy and that of the European, exhibit a trend bias than the others.

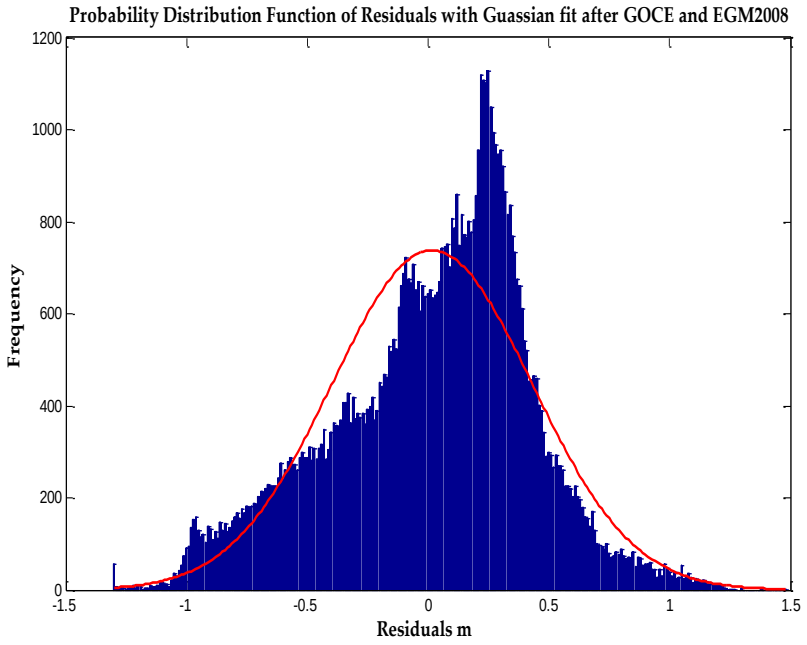

Figure 4.17: Probability Distribution Function of the residuals

max	**1.486m**
min	-1.613
Mean	0.0166m
STD	0.414m
Variance	0.171m

Fig: 4.3 Stat. of Residuals

4.4.3 Constant with a Common Trend Bias Removal

Due to the small size of the individual area under consideration, the translation of the barycentre takes into account the mean radius of the Earth, which affects the estimating parameter. The effect of the Earth dimension on the trend cannot be ignored, especially in the case of

Switzerland, of an area 23km sq compared to the Earth radius. To solve the problem of the border effects taking into consideration the radius of the Earth, the best way is to estimate a constant bias for each quasigeoid and a common trend for all three excluding the European quasigeoid due to the large border jumps it shows. This approach will combine the constant value in each quasigeoid with a trend by reducing the contributing factor of the Earth radius on the estimated parameters. Here the formulation considers the origin for each model and a common translation of the barycentre of all three.

$$B_i = a_i + b_i \cos\Phi \cos\lambda + c_i \cos\Phi \sin\lambda + d_i \sin\Phi + v1 \qquad (4.9)$$

Where a_i is the origin of the geoids and b, c, d, is the same translation of the barycentre for the three models and *i* for each geoid. Therefore the design matrix for the estimation is given as for i = Italy, Switzerland, French,

$$\Delta = \begin{bmatrix} B_{it} & \emptyset & \emptyset & \emptyset \\ \emptyset & B_{ch} & \emptyset & \emptyset \\ \emptyset & \emptyset & B_{fr} & \emptyset \\ \emptyset & \emptyset & \emptyset & B_{eu} \end{bmatrix} \quad \text{m x 6} \qquad X = \begin{bmatrix} a_i \\ b \\ c \\ d \end{bmatrix} \quad \text{6 x 1} \qquad Q_{error} = \begin{bmatrix} \sigma^2 & \cdots & c(\psi) \\ \vdots & \ddots & \vdots \\ c(\psi) & \cdots & \sigma^2 \end{bmatrix} \quad \text{m x m} \qquad (4.10)$$

The observation equation, herein being the residuals after removing the low and high frequencies is a column vector of m observations.

$$r = \begin{bmatrix} \delta N_{iti} \\ \vdots \\ \delta N_{chi} \\ \vdots \\ \delta N_{fri} \end{bmatrix} \quad \text{m x 1}$$

From least squares the parameters x is given by $x = \left(\Delta^t * Q^{-1}{}_{er} * \Delta\right)^{-1} * \left(\Delta^{-1} * Q^{-1}{}_{er} * r\right)$

$Q_{er} = C_{GOCE} + C_{EGM2008} + C_{vv}$ where C_{vv} is considered white noise of the local geoid model. The figure 4.18 shows the new bias approach of a separate constant and a common trend for all models.

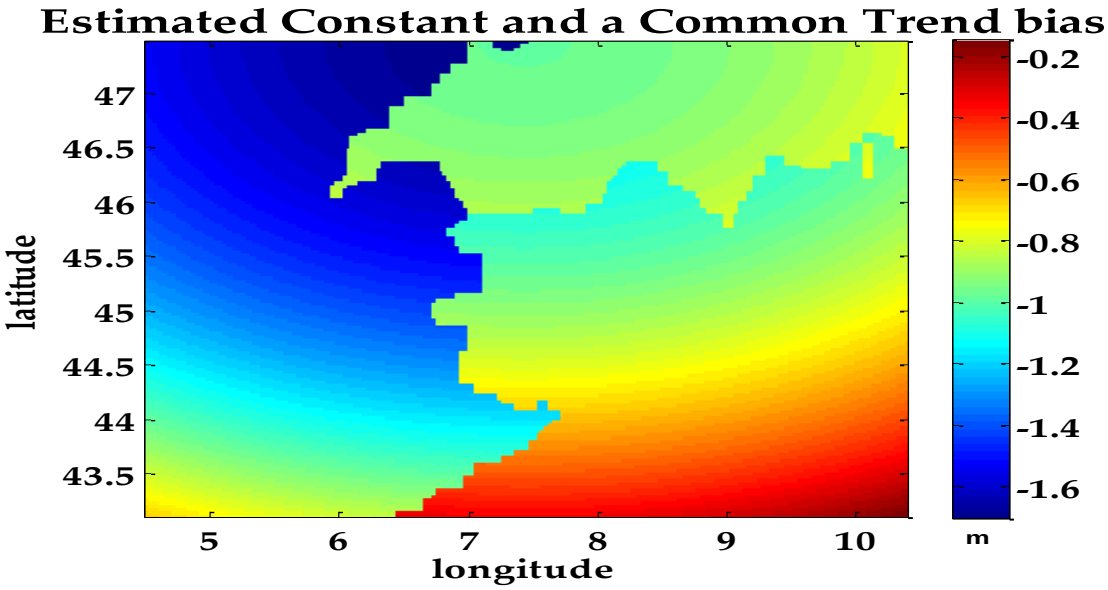

Figure 4.18: Constant parameters with common trend bias

The removal of the new bias estimation gives a better border effect solution compared to the previous estimation approaches. Here the jumps at the boundaries are not visible for most of the boundary length as shown in figure 4.19 with a corresponding histogram of the final very high frequencies (residuals) in figure 4.20. Though the histogram is still skewed as in the constant bias removal, the statistics gives a better result. This procedure combines the merits of the previous two bias estimation approaches.

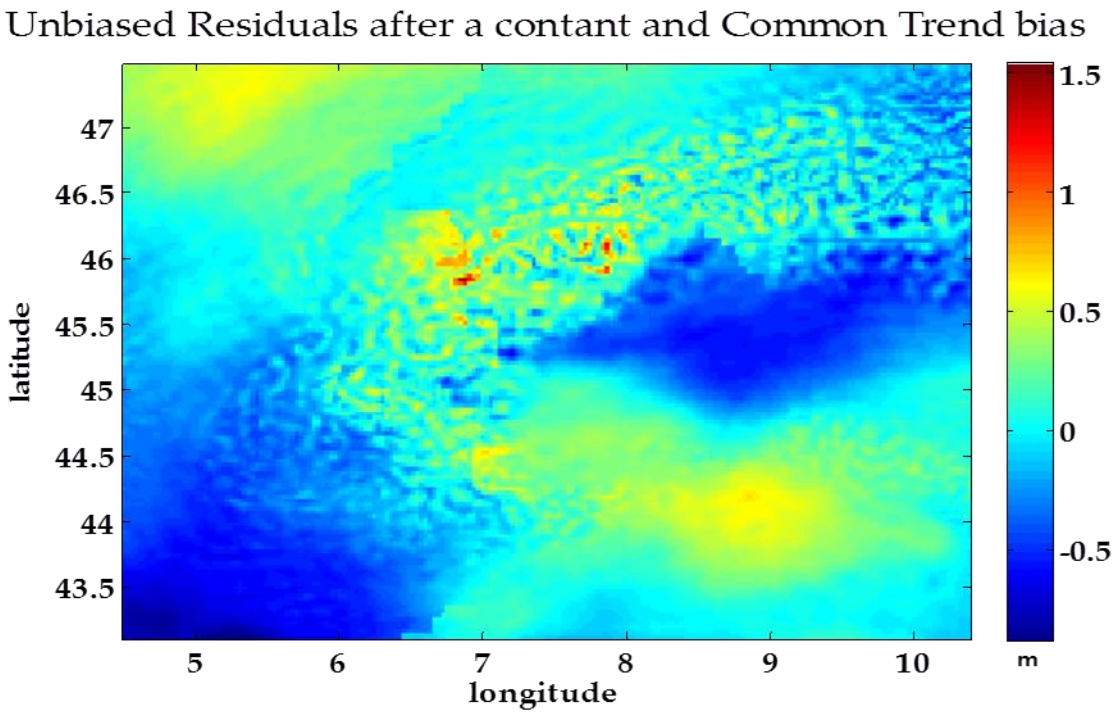

Figure 4.20: Unbiased residuals after a constant with common trend removal

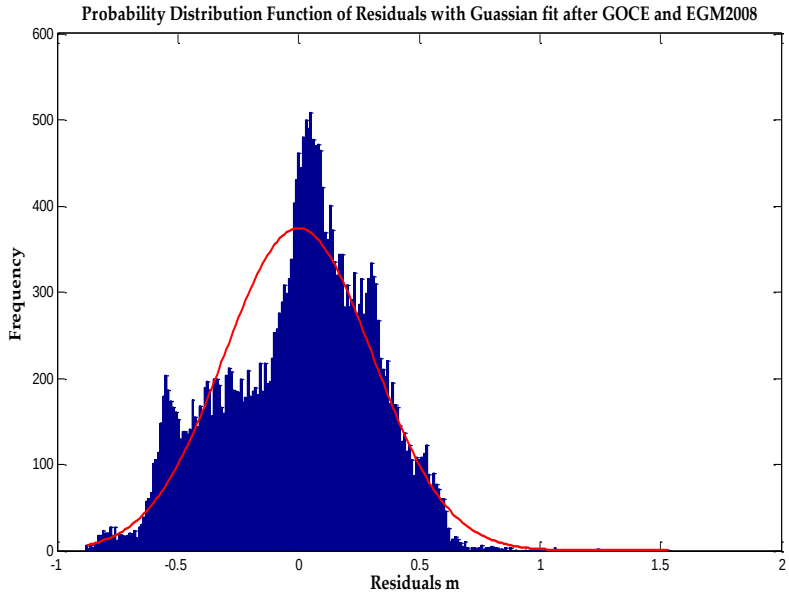

Figure 4.21: Probability Distribution Function of the residuals

max	1.54 m
min	-0.87 m
mean	-3.3e-4 m
var	0.09 m
std	0.31 m

Fig: 4.4 Statistics of the Residuals

The figure 4.22 shows the final quasigeoid after removing the bias and putting back all the signals from GOCE and EGM2008. Comparing with the biased model and the differential in latitude direction, it can be seen that most of the jumps has been taken care off.

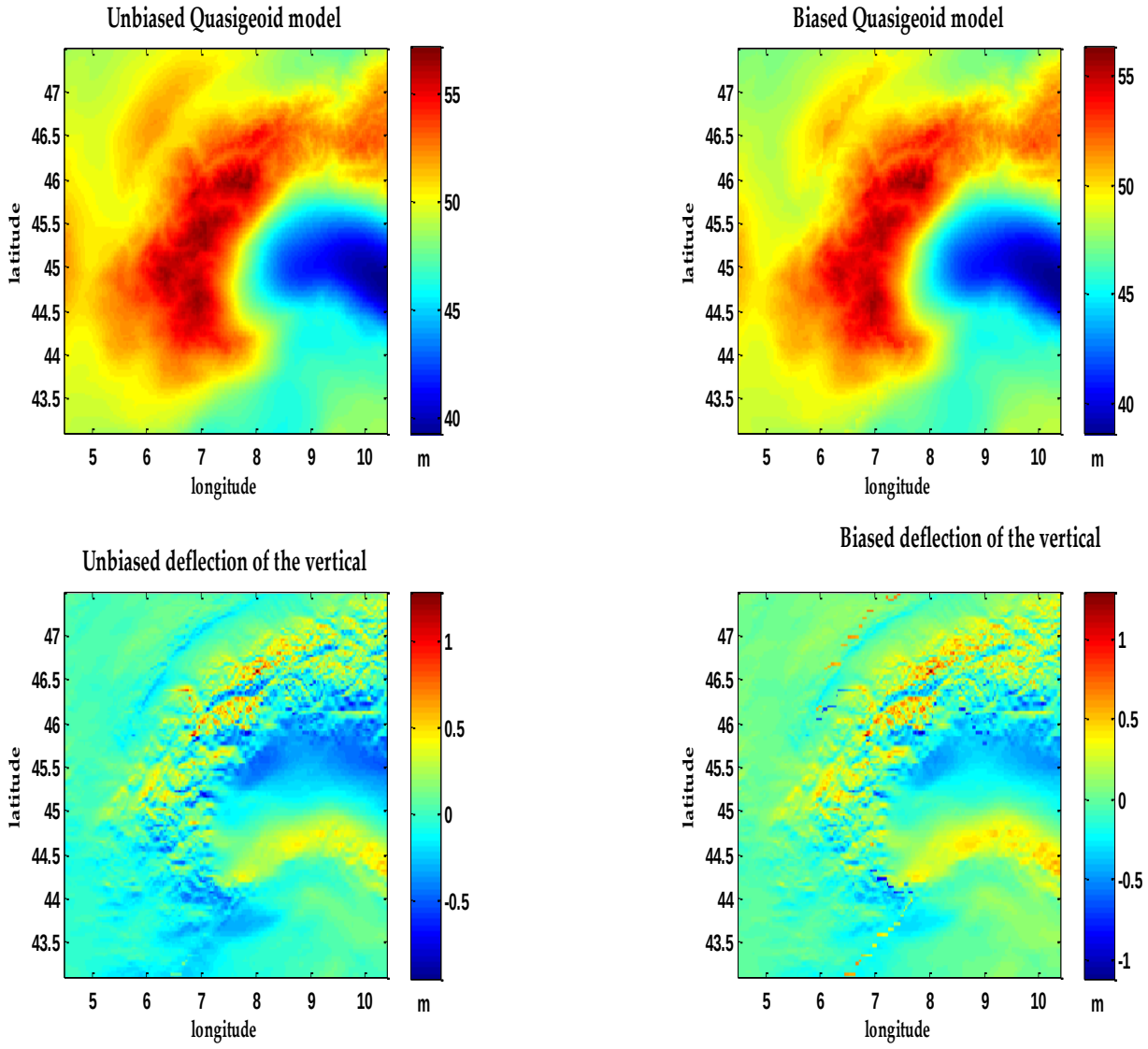

Figure 4.22: Image comparison of biased and unbiased model with the vertical deflection

4.5 Boundary Merging

The main objective of this research is to align the quasigeoid without discontinuities along the borders, such that civil engineering works or height transfer across the national boundaries will not contain bias. Removing the biases with satellite global gravity models is the first step to the solution, but to have a smooth model across the borders is the final goal of the work. There is therefore the need to employ a proper statistical procedure for the boundary merging of the unbiased quasigeoid. This can be achieved by using any of these statistical methods, least squares, collocation and Kriging to merger the borders with the other.

4.6 Boundary Interpolation with Kriging

Assuming the unbiased residuals (i.e. high frequencies due to topography), by Wiener-Kolmogorov (WK) theory, as a homogenous and isotropic field (Eq. 4.6), stationary in both time and space, a prediction with Kriging is made at the borders of neighbouring countries by know the empirical variogram and the model variogram. This was done by building a moving window, which takes observations from both sides of the border in order to build the prediction.

$$r_i = \boldsymbol{v}(t_i) + v_i \tag{4.11}$$

Given as the noise E[$\underline{v}$] = 0, $C_{vv} = \sigma_v^2 I$ is a white noise and the signal E[v(t)] = 0, E[v(t) v(t +τ)] = $C_v(\tau)$, as the covariances. Hence assuming the prediction at the boundaries u, (i.e. linear combination of $\underline{\hat{u}}(t) = \underline{\lambda}^+ \underline{r}$) having a constant mean μ different from zero; $u(t) = \mu + v(t)$ the observation equation is expressed as

$$\underline{r} = \mu \underline{e} + \underline{\boldsymbol{v}} + \underline{v} \tag{4.12}$$

Where $\underline{e}$ is a column vector with all elements equal to 1, and from the covariance structure, the variogram is given as $\gamma(\tau) = C(0) - C(\tau)$. (i.e. $(t, t') = \frac{1}{2} E\{[u(t) - u(t')]^2\}$), where t = (Φ_i, λ_i) and t' = (Φ_j, λ_j). The sample variogram and the variogram fit for the boundary prediction were built with a moving window, of a lag distance of about 2.5°. Observations on both sides of the prediction point were used in the variogram estimation. Figure 4.8 and 4.9 show the borders to be predicted.

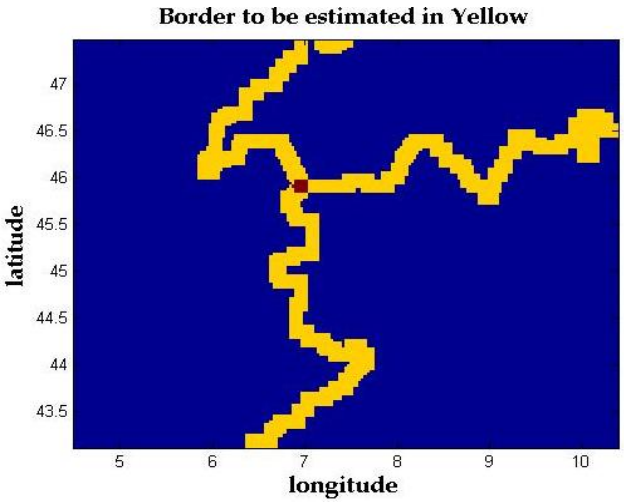

Figure 4.23: Outline of border between countries

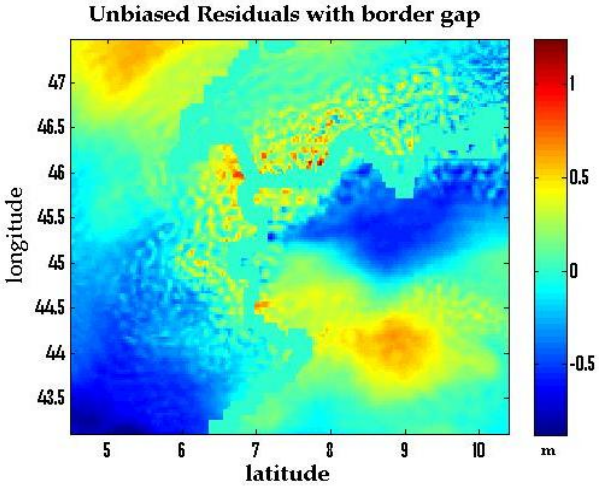

Figure 4.24: Outline of border between the countries for the geoid residuals

The moving window was built such to partition the area into three parts, to see the individual variograms (covariance), for the assumption of a homogenous and isotropic field. All the three variograms were similar; hence the prediction assumption was met. Figure 4.10 shows the three variograms, for each the model variogram synthesized from the data and the variogram fit with their corresponding prediction at the borders.

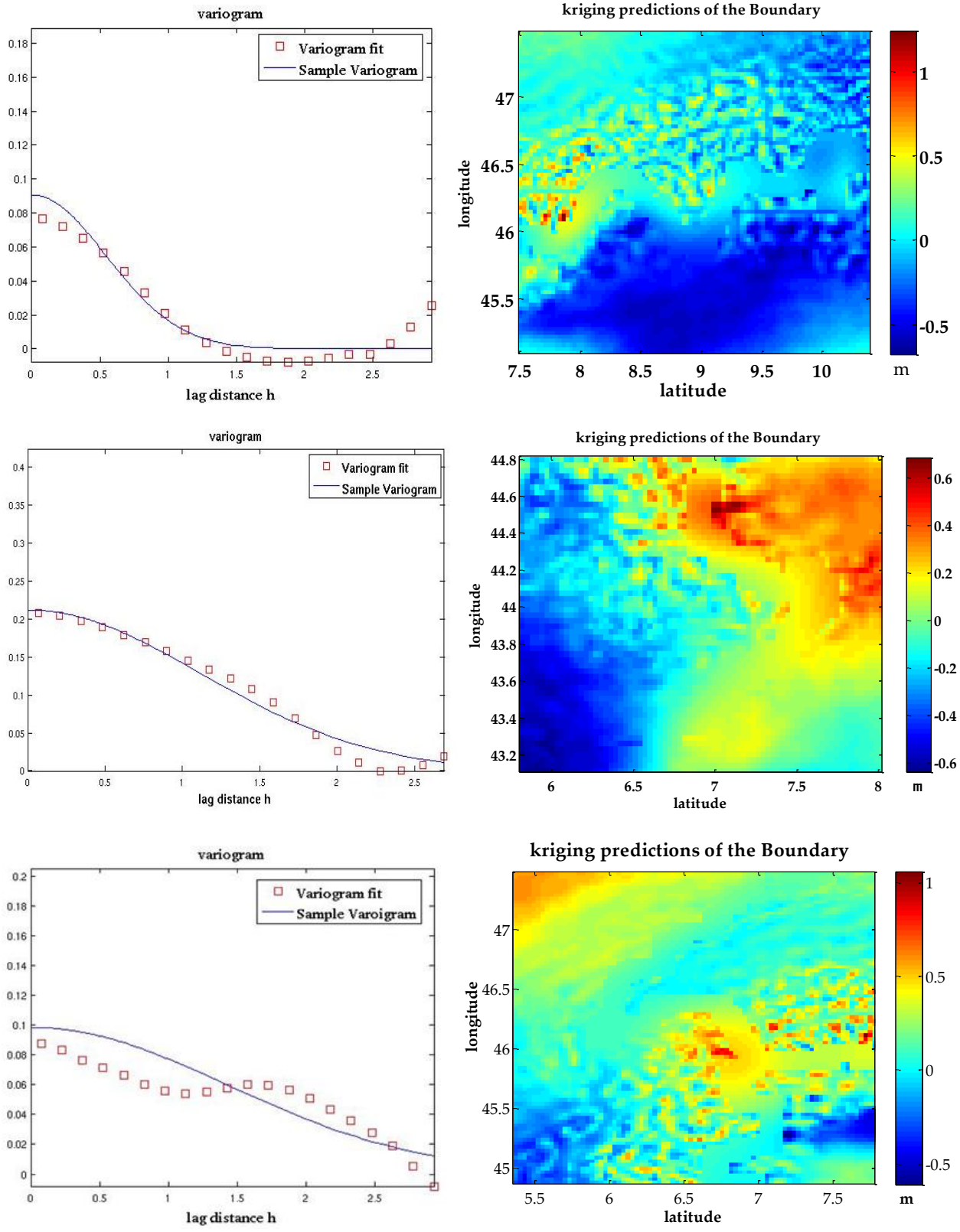

Fig: 4.10 Variogram and prediction of the boundary.

Figure 4.11, shows the merged quasigeoids of the three countries. The topographic effect is still present, contributing to the very high frequencies. The next best step is to have terrain correction to correct the effect of the topography, before adding back the frequencies taken out by the global models; GOCE and EGM2008. Adding back the signals from both GOCE and EGM2008 give the final map shown in figure 4.12.

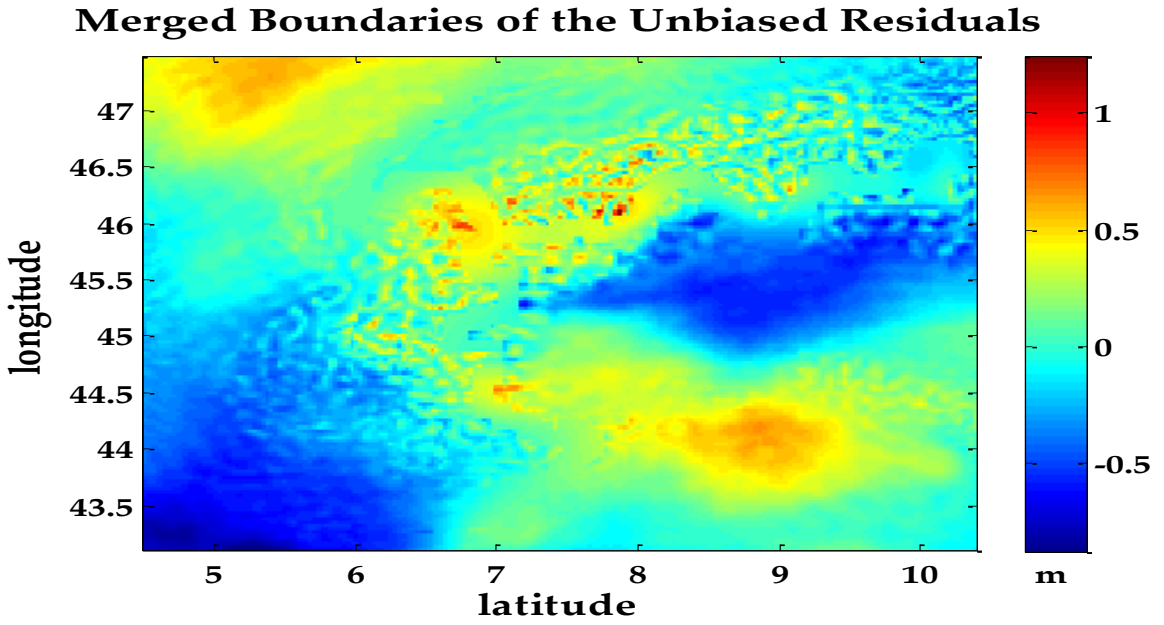

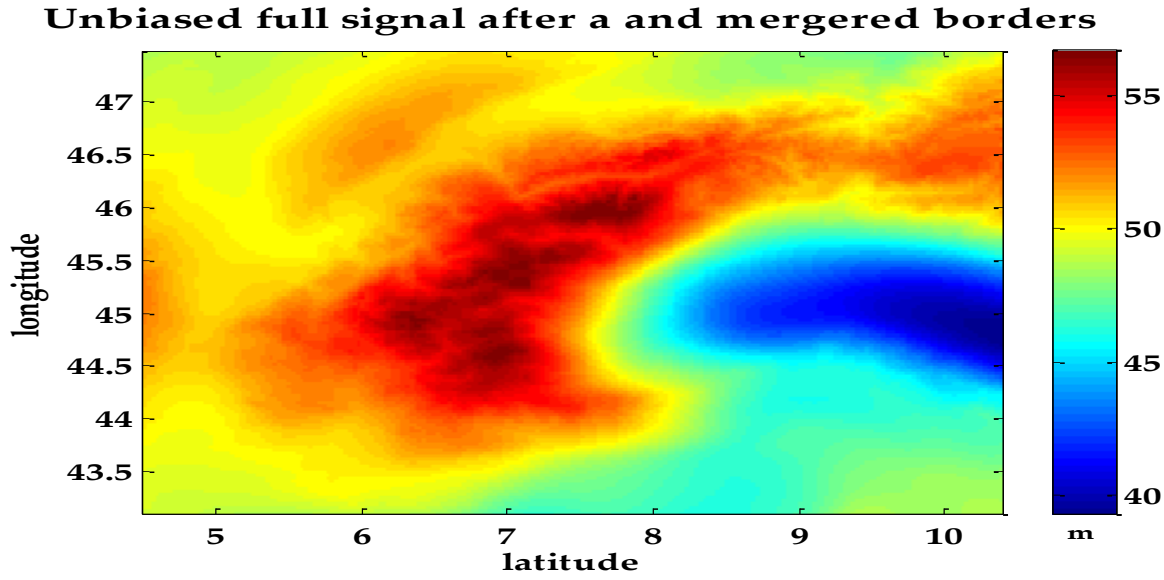

The use of the moving window for the Kriging prediction uses just considers small portion of the observations within the lag distance. Further investigation of the shape of the variogram, in case a one-step computation of the boundaries was done, but due to the computation limitation of the computer capacity, the residuals were down sampled from 146x197 to 73x99. Here each predicted border value is affected by all the observations. The shape of the sample variogram and the variogram fit is not very much different from that of the moving window.

Chapter 5

5.0 Evaluation of the Results with GPS levelling

5.1. GPS levelling

Nowadays it is possible to measure geoid undulation with very high accuracy from ellipsoidal height observed by using GNSS (Global Navigation Satellite System) technologies and orthometric height traditionally derived from levelling data and gravity measurements. In fact GPS measurements can be taken at benchmarks with known orthometric height H and the difference between the GPS-derived ellipsoidal height h and the orthometric height H provides the geoid undulation $N_{h\text{-}H}$ at the observed point as shown in equation 5.1 and Figure 5.1:

$$N_{h\text{-}H} = h - H. \qquad (5.1)$$

Note that since GNSS derived height and orthometric height can be observed, a part for a constant, with accuracies of few millimetres this technique will give high reliable geoid undulations. Unlike the gravimetric geoid, the N value is confined only to the observed position, which has to be extrapolated to cover the entire region of interest. Hence such model is only valid with millimetres accuracy over the area encompassed by the known benchmarks. The gravimetric geoid estimation gives uniform grid of geoid undulation over large area in contrast to the GPS scattered values over small area. Comparing the values of GPS geoid undulation to gravimetric geoid for the same region therefore needs interpolation of the gravity geoid in the respective GPS-levelling position.

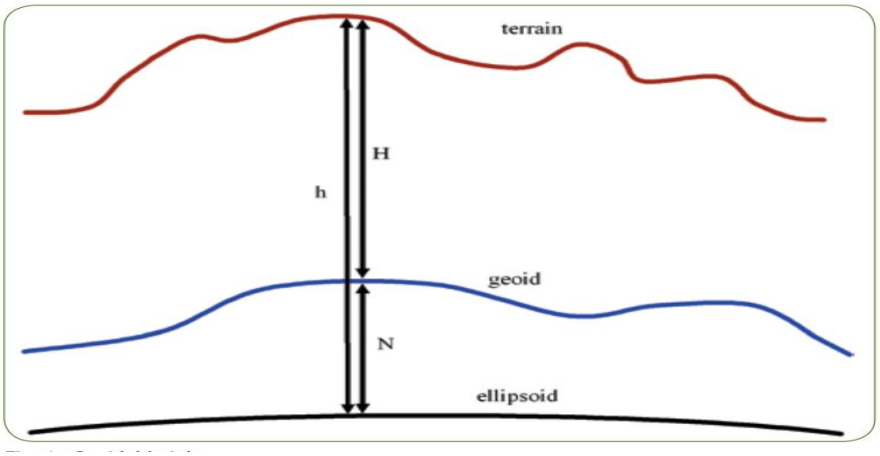

Figure 5.1: GPS-levelling geoid height

5.2. Comparison of the final merged Quasigeoid with GPS levelling

The GPS-levelling geoid height $N_{h\text{-}H}$ can be used as an independent source in validating the gravimetric geoid N to infer the combined quality of satellite and terrestrial gravity data.

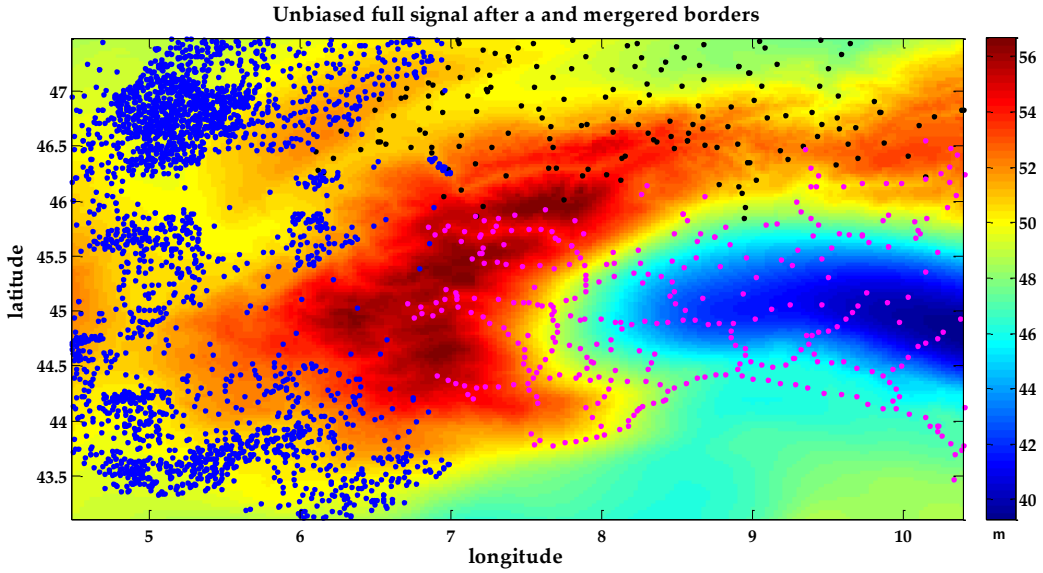

Figure 5.2: GPS levelling geoid in points overlaid on gravimetric geoid

The discrepancies between them represent errors in the gravimetric geoid undulation, in the interpolation from the original grid to the GPS-leveling points as well as in *h* and *H*.

In detail the first error, i.e. the errors in the gravimetric geoid undulation are in the range between 10 cm for the Italian geoid and 2-3 cm for the swiss one. The second term, i.e. the interpolation error, can be estimated by interpolating from the original grid the geoid undulation at a grid knot (considered unknown) and by comparing the interpolated value with the original one. In the considered area this error is of the order of 6 cm (standard deviation). As for the errors in *h* and *H* they are of the order of few centimetres (2-3 cm standard deviation). For the three national geoids finally aligned, networks of GPS were used to determine the scattered δN values for respective area. Due to the fact that orthometric height are computed starting from different zero levels for each nation there is an intrinsic bias in each set of N_{h-H} values.

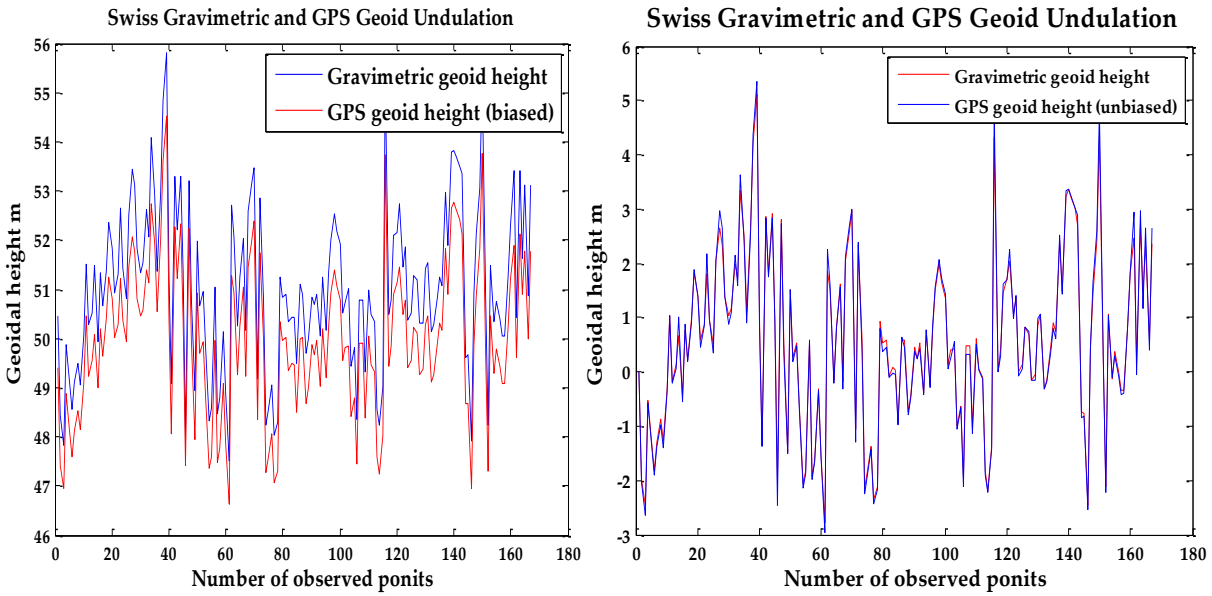

Figure 5.3: Plot Gravimetric with biased and unbiased GPS derived N for Swiss

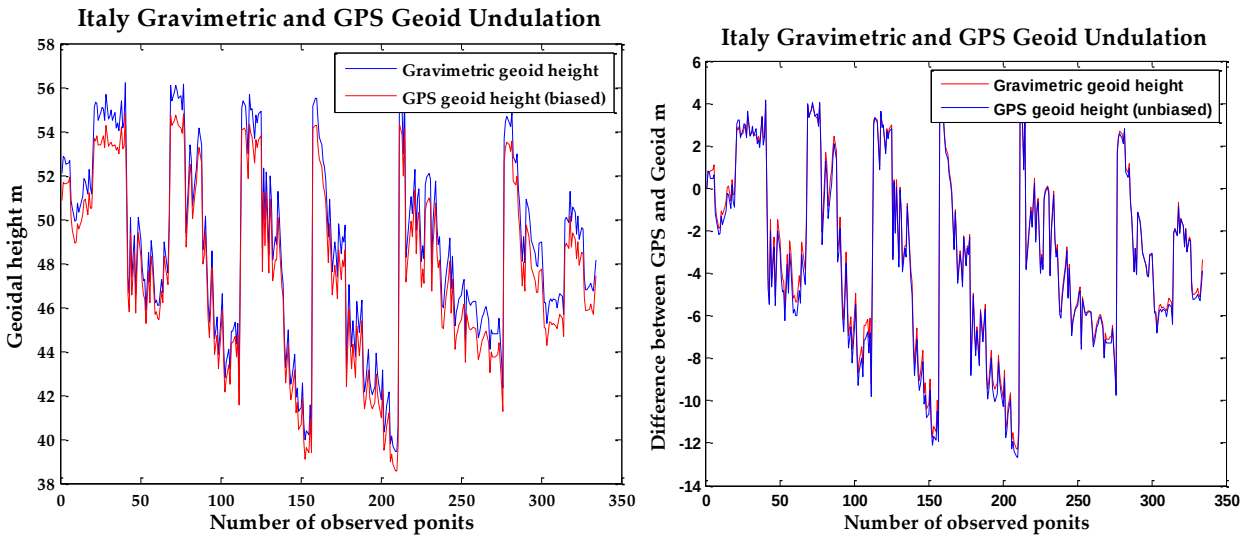

Figure 5.4: Plot Gravimetric with biased and unbiased GPS derived N for Italy

The computed geoid is a grid of resolution 3' x 3' which is approximately 5km square. Comparing the model with GPS geoidal height which has the full signal at the observed station the residuals statistics is report in table 5.1. The standard deviation is the contribution of the error of the local geoids, interpolation error and error from the GPS levelling. Figure 5.3 shows the histogram representation of the residuals from the comparison of the computed model with GPS levelling heights.

Statistics	Swiss	Italy
Mean	1.5 cm	25 cm
Standard Deviation	14 cm	22 cm
Maximum	45 cm	74 cm
Minimum	-51 cm	52 cm

Table 5.1: Statistics of the difference between GPS and gravimetric geoid

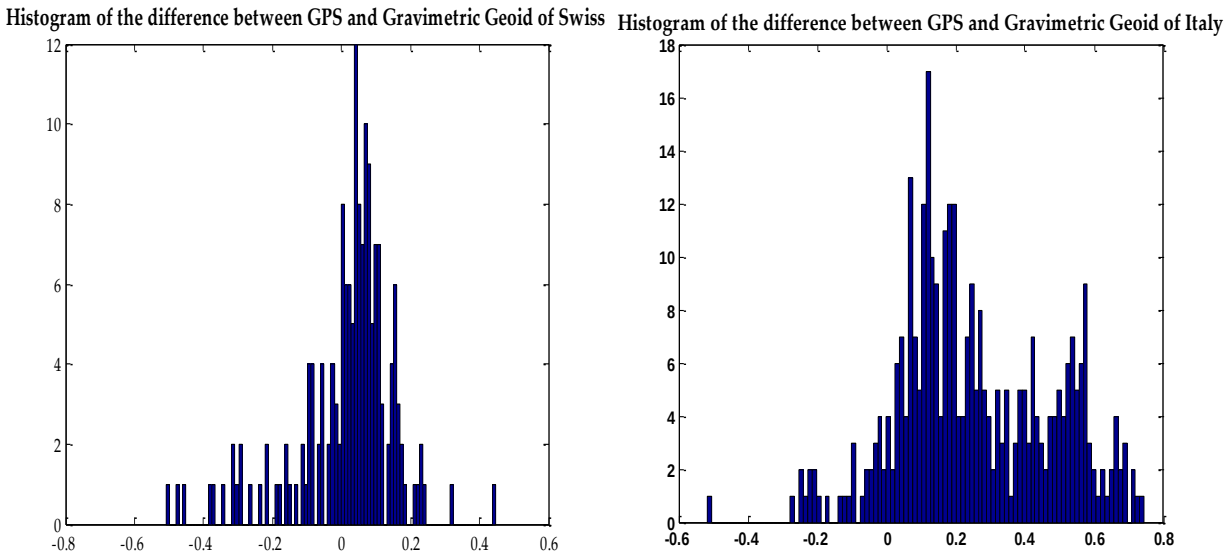

Figure 5.5: Histogram of residual s from GPS and Computed model for Swiss and Italy

The figure 5.6 shows a cross section view plot of geoidal height along one longitude for the biased and unbiased model and the arrows indicates some of the border effects (jumps).

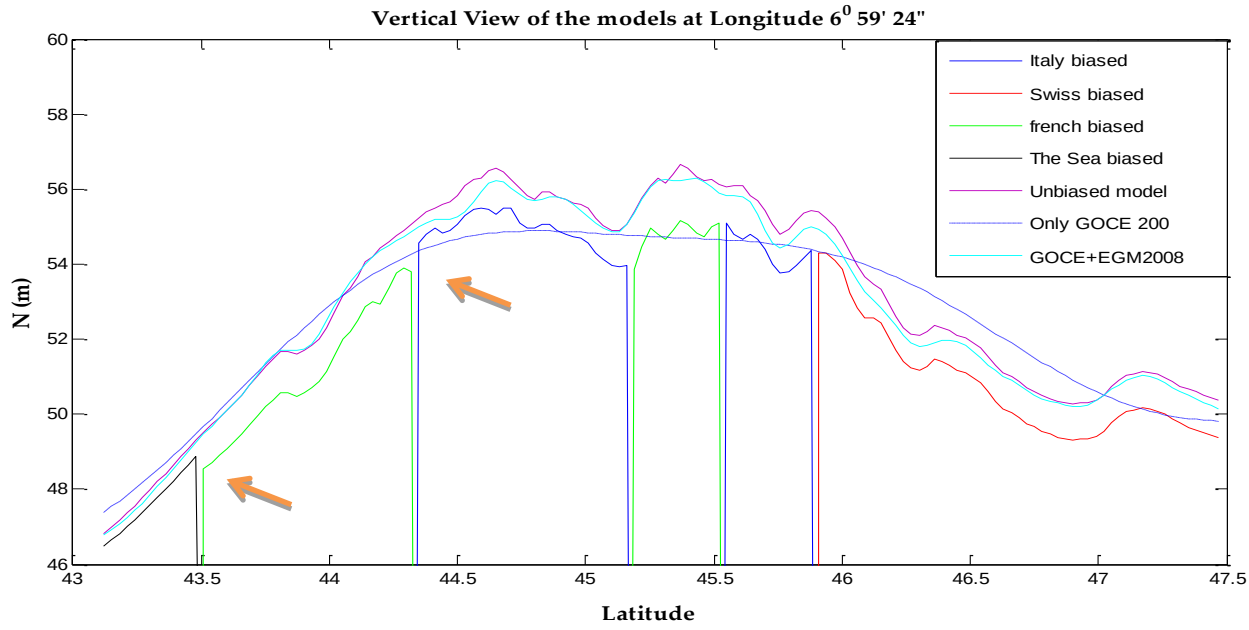

Figure 5.6: vertical section of the different geoid models

Chapter 6

6.0 Conclusion

The research sorts to merge local geoids shearing boundaries by removing the biases of each local geoid. In fact due to the presence of these biases, there are systematic effects at the borders which give problem in orthometric height transfer across countries. In particular this study represents a first investigation on the way different local geoids can be merged using GOCE data. Even if the cleanest way to produce an unbiased local geoid is to merge GOCE gravity gradients with terrestrial gravity measurements, the explained procedure can be useful to merge already available local geoids without repeating all the computations from the original observations that, by the way, are not always of public domain. A two-step solution to merge local geoids has been studied and implemented. The whole procedure has been applied to compute an unbiased unique geoid in the Alpine region. We tried to compute the bias by investigating three different "shapes" for the bias model has been investigated, i.e. a constant for each local geoid, a constant and a trend for each local geoid and a constant for each geoid plus a unique trend in the considered region. The modelling that seems to work better, i.e. that minimizes the border effects, is the one made by a single trend and a constant for each local model. Even, once the bias have been removed, there are still small residuals and local border effects present in the data. These effects can be removed by Kriging interpolation at boundary.

The whole procedure has been applied at one of the most critical areas; the Alpin region in Europe giving promising results: in particular it leads to estimate the biases with an

accuracy of the order of few centimetres and an unified unbiased geoid with an accuracy comparable with the one of the original gravimetric models. In other words the height datum problem at the local level has been solved. The mean of the Swiss geoid compared with GPS levelling is of 1.5 cm, which is within the range of expected value, unlike the Italian mean value 25 cm which can be the results of the procedure used: the unique trend estimated over the whole region in fact leads to a non zero mean in the Italian region. The standard deviations are within the expected values, at the considered resolution, considering the contributions of all the respective errors; Swiss (i.e. 10 cm against 14 cm) and Italy (i.e. 20 cm against 22 cm).

In a recommendation, Future works should explore high data GOCE model the better the solution achieved with six months GOCE data model. Likewise the terrain effect should be dealt with to give a better resolution for the Kriging procedure. This preliminary study solved the problem of computation with the large data size by down sampling; hence future works should investigate how the whole data set can affect all computation of the potential field. The best fit bias computation used, attributed to the high value of the mean value of the Italian geoid compared to the four parameter estimation, hence there is the need for studying how the topographic trend affect the bias estimation method. Finally it has to be stressed that the dimension of the area considered is an important factor in the estimate of the bias. When the area is large enough it is probably not necessary to subtract the high frequency signal contribution of EGM2008, but it is sufficient to subtract a GOCE-only geoid. This at least seems to result from a preliminary analysis that will be the object of future researches.

1.0 Reference

1. Allister, N.A. and Featherstone, W.E. (2001) Estimation of Helmert orthometric heights using digital barcode levelling, observed gravity and topographic mass-density data over part of the Darling Scarp, Western Australia, Geomatics Research Australasia, No. 75, pp. 25-52.
2. Amos, M.J. (2007) Quasigeoid Modelling in New Zealand to Unify Multiple Local Vertical Datums pp. 10-11
3. Barzaghi R, Borghi A, Carrion D, Sona G (2007) Re_ning the estimate of the Italian quasi-geoid. Bollettino di Geodesia e Scienze A_ni 66(3)
4. Colombo, O.L., 1981. Numerical Methods for Harmonic Analysis on the Sphere. Report No. 310, Department of Geodetic Science, The Ohio State University, Columbus.
5. Denker, H., Behrand, D. and Torge, W. (1996) The European gravimetric quasigeoid EGG95, in: Sansò, F. (Ed.) New geoids of the world, International Geoid Service Bulletin, 4, Milano, Italy, pp. 3-12.
6. Dennis, M.L. and Featherstone, W.E. (2003) Evaluation of orthometric and related height systems using a simulated mountain gravity field, in Tziavos I.N. (Ed.) Gravity and Geoid 2002, Ziti Editions, Thessaloniki, Greece, pp. 389-394.
7. Duquenne H. (1997), The French quasigeoid, International Geoid Service depository, www.iges.polimi.it
8. Featherstone, W.E. and Kuhn, M. (2006) Height systems and vertical datums: a review in the Australian context, Journal of Spatial Science, Vol. 51, No. 1, pp. 21-41
9. Featherstone, W.E. (2004) Evidence of a north-south trend between AUSGeoid98 and AHD in southwest Australia, Survey Review, Vol. 37, No. 291, pp. 334-343.

10. Forsberg R. (1994) Terrain Effects in Geoid Computations. In Lecture Notes "International School of the Determination and Use of the Geoid", October 1994, pp:149-182, Milan, Italy.
11. Heck B. (2003) On HelmertS method of condensation. Journal of geodesy, DOI 10.1007/s00190-003-0318-5
12. Gatti, A., Reguzzoni, M., & Venuti, G. (2013). The height datum problem and the role of satellite gravity models. Journal of Geodesy, 87(1), 15-22. DOI 10.1007/s00190-012-0574-3
13. Heiskanen, W.A. and Moritz, H. (1967) Physical Geodesy, W.H. Freeman and Company, San Francisco, USA, 364 pp.
14. Hipkin, R.G. (2000) Modelling the geoid and sea surface topography in coastal areas, Physics and Chemistry of the Earth, Vol. 25, No. 1, pp. 9-16, doi: 10.1016/S1464-1895(00)00003-X.
15. Hofmann-Wellenhof, B., & Moritz, H. (2006). Physical geodesy. Springer.
16. Jekeli C, Potential Theory and Static Gravity Field of the earth, 2007
17. Kearsley AHW and Forsberg R (1990) Tailored geopotential models - applications and shortcomings. Manuscripta Geodetica, 15(3):151-158
18. Klees R., Tenzer R., Prutkin I., Wittwer T. (2008) A data-driven approach to local gravity modelling using spherical radial basis functions. Journal of Geodesy, 82(8), 457-471.
19. Krarup T. (2006) A convergence problem in collocation theory. Borre K (ed) Mathematical foundation of geodesy. Springer, Berlin
20. Martinec Z. and Vanicek P. (1994) Direct topographical effect of Helmert's condensation for a spherical approximation of the geoid. Manuscripta Geodetica, 19(5):257-268

21. Melchior, P. (1981) The Tides of the Planet Earth, Pergamon Press, Oxford, England, 655 pp.
22. Merry, C. and Vaníek, P. (1983) Investigation of local variations of sea surface topography, Marine Geodesy, Vol. 7, No. 2, pp. 101-126
23. Molodenskii MS, Eremeev VF, Yurkina MI (1962) Methods for study of the external gravity field and figure of the Earth. Israel Program of Scientific Translations, Jerusalem (Russian original 1960).
24. Moritz, H., & Mueller, I. I. (1987). Earth rotation: theory and observation. New York: Ungar, 1987., 1.
25. Moritz H. (1980) Advanced Physical Geodesy. Wichmann H, Karlsruhe, Germany.
26. Marti U. (2004), CHGeo2004Q, Switzerland quasigeoid, international geoid service depository, www.iges.polimi.it
27. Novak P. (2007) Gravity reduction using a general method of Helmert's condensation. Acta Geodaetica et Geophysica Hungarica. 42(1):83-105.
28. Pail, R., Bruinsma, S., Migliaccio, F., Förste, C., Goiginger, H., Schuh, W. D., ... & Tscherning, C. C. (2011). First GOCE gravity field models derived by three different approaches. Journal of Geodesy, 85(11), 819-843.
29. Pavlis N. K. The Development and Evaluation of the Earth Gravitational Model 2008 (EGM2008)
30. Pugh, D. (2004) Changing Sea Levels: Effects of Tides, Weather and Climate, Cambridge University Press, Cambridge, United Kingdom, 265 pp
31. Reguzzoni, M., 2004. GOCE: the space-wise approach to gravity field determination by satellite gradiometry. PhD Thesis, Politecnico di Milano, Italy.
32. Reguzzoni M. First GOCE gravity field models derived by three different approaches, 2010

33. Reguzzoni M, Sampietro D and Sanso F (2011) Updating EGM08 Mediterranean Geoid Using Local GOCE Data from the Space-Wise Solution. In: Proc. of the 4th International GOCE User Workshop, 31 March - 1 April 2011, M□unich, Germany, ESA SP-696. ISBN: 978-92-9092-260-5, ISSN:1609-042X
34. Barzaghi R, (2005), Italian quasigeoid computed at Politecnico di Milano, International geoid service depository, www.iges.polimi.it
35. Sansò F. (1986) Statistical methods in physical geodesy. Snkel H (ed) Lecture notes in Earth sciences, Mathematical and Numerical Techniques in Physical Geodesy, 7:49-155, Springer, Berlin
36. Sansò F., Sideris MG. Geoid Determination: Theory and Methods. Springer, 2013.
37. Sansò, F. and Vanícek, P. (2006) The orthometric height and the holonomity problem, Journal of Geodesy, Vol. 80, No. 5, pp. 225-232, doi: 10.1007/s00190-005-0015-7
38. Stokes GG (1849) On the variation of gravity at the surface of the Earth.
39. Torge, W. (2001) Geodesy, 3rd Edition, Walter de Gruyter, Berlin, Germany, 416 pp
40. Tscherning C.C. (1994) Geoid Determination by Least-squares Collocation Using GRAVSOFT. Lecture Notes "International School of the Determination and Use of the Geoid", October 1994, pp:183-213, Milan, Italy
41. Vanícek, P., Castle, R.O. and Balazs, E.I. (1980) Geodetic levelling and its applications, Reviews of Geophysics and Space Physics, Vol. 18, No. 2, pp. 505-524.
42. Vannicek P. and Sjoberg L.E. (1991) Reformulation of Stokes's theory for higher than second degree reference field and modification of integration kernels. J. Geophys. Res., 96(B4): 6529-6539

43. Wenzel HG (1982) Geoid computation by least squares spectral combination using integral kernels. In: Proceedings of the IAG General Meeting, Tokyo, pp:438-453.